Study of Radar Signal Attenuation in Dust Storms

Prepared by:

Saad I. Alhuwaimel

ALHSAA001

Supervised by:

M. R. Inggs

Department of Electrical Engineering

December 2012

A dissertation submitted to the Department of Electrical Engineering,

University of Cape Town,

in partial fulfilment of the requirements

for the degree of

Master of Engineering specialising in *Radar*.

Declaration

1. I know that plagiarism is wrong. Plagiarism is to use another's work and pretend that it is one's own.
2. I have used the IEEE convention for citation and referencing. Each contribution to, and quotation in, this project report from the work(s) of other people, has been attributed and has been cited and referenced.
3. This project report is my own work.
4. I have not allowed, and will not allow, anyone to copy my work with the intention of passing it off as their own work or part thereof.

Signature of Author .....

Cape Town
21 December 2012

Abstract

The prediction of electromagnetic propagation through dust clouds assumes greater importance due to the increased use of microwave communications and radar in those parts of the world where these storms are found.

This project reviews the morphological and electrical properties of the dust and its distribution in a dust storm. Dust cause attenuation and phase shift in the propagating electromagnetic waves. Eight mathematical attenuation and phase shift prediction models from the literature are presented. The attenuation predictions only are analysed. It was found there are huge differences between the predicted and the measured attenuations. One reason that might justify this difference is the induction of charge on the dust particles in wind-blown dust storms. This charge is known to increase the attenuation. We conclude that a great deal of further experimental work is required.

Acknowledgements

I would like to thank my supervisor, Michael Inggs, and Dr. Amit Mishra for excellent guidance given throughout the project. I thank my parents and my wife for their support.

Contents

List of Figures

List of Tables

List of Symbols

M	—	Dust particles mass concentration
ρ	—	Dust density in a dust storm
V	—	Visibility
r	—	Dust particle radius
r_{av}	—	Average dust particles radii
r_e	—	Effective dust particles radii
v	—	Relative volume fraction of the air occupied by dust storm
A_i	—	Depolarization factor
α	—	Dust particle size parameter
α_0	—	Optical attenuation
A	—	Attenuation
Φ	—	Phase shift
Γ	—	Propagation constant
δ	—	Depolarization angle
XPD	—	Cross-polarization discrimination
L_d	—	Depolarization loss

Nomenclature

Sand—fine grains or granular material that occurs naturally and composed of finely divided rock and mineral particles. The radius of sand grain ranges between 50μm to 2mm.

Dust—tiny particles in the atmosphere that come from various sources such as soil dust lifted by wind or feather, volcanic eruptions, and pollution. The main composites of the dust are: silt (radius: 2um to 50 um) and clay (radius: less than 2μm).

Sand/Dust storm—A dust storm or sand storm is a meteorological phenomenon where a gust front or other strong wind blows the loose sand and dust particles from dry surface, transport them from one place and deposits them in another place. This storm is common in arid and semi-arid regions.

EMW—Electromagnetic wave.

EM—Electromagnetic.

Monodispersive—: Monodispersive medium is the medium that has particles all having the same size.

Polydispersive—: Polydisperse medium is the medium that contains particles of more than one size.

Dusty medium—: Air with at least 80% of the weight of the suspended particles have radii less than 35μm.

Visibility—: The distance that human eye can see through dust storm.

Depolarization factor—: The ratio of the internal electric field induced by the charges on the surface of a dielectric when an external field is applied to the polarization of the dielectric.

Depolarization angle—: The angle difference between the propagating wave angle of incidence on non-spherical dust particles in a dusty medium and the wave angle after passing through the medium.

Cross-polarization discrimination—The ratio of the power received at the reception point in principal polarization of the incident wave to that received in orthogonal polarization of the same incident wave.

Chapter 1

Introduction

The earth surface in arid and semi-arid regions is permeated with sand and dust particles that can be blown by the air flow. The wind-blown sand and dust constitute the sand/dust storms.

The particle sizes form the main difference between the sand and dust. In the literature, sand particles are known to have radii that fall in the range 50 μm to 2 mm. On the other hand, dust particles are known to have radii of less than 50 μm. Due to sand particles large size, and hence their weight, it becomes difficult for the blowing wind to elevate them to more than few metres, rarely above 2 m as reported by Chu [15] and Ansari and Evans [8]. However, the light weight of the dust particles assists the blowing wind to elevate them to a greater height, up to 5 km as reported by Norinpel [16], compared to sand particles. Figure 1.1 serves as an example of s dust storm height in Riyadh, Saudi Arabia. In this report, the terminology *Dusty medium* is used to indicate air with suspended dust particles.

The number of dust storms is increasing in the Middle East and North Africa, as reported by Al-Dabbas et al. [17] and Elshaikh et al. [18]. Figure 1.2 shows the increasing number of dust storms in Khartoum, Sudan in 2006 compared to 1997 [18]. This has led to an increase in the importance of studying the effects of dust storms on wireless communication, especially the one that utilises

Figure 1.1: February 2012 Dust storm - Riyadh, Saudi Arabia. The tower in the photo is the Kingdom Tower, which is 300 meter high. (www.americanbedu.com)

long-distance traveling waves, such as radar.

1.1 Background

The utilization of electromagnetic wave (EMW) applications in the areas experiencing dust storms has increased the importance of studying and, quantitatively, predicting the effects of dust storms on these applications. The propagation of an EMW in a dusty medium can be hampered when the wave interacts with the dust particles. This interaction will result in attenuating the propagating EMW which form the main effects of dust storms on the electromagnetic waves. The attenuation is also called extinction [19].

Scattering and absorption are the two main physical mechanisms that form the main causes of the attenuation that occur to a propagating EMW in a dusty medium. The extinction (attenuation) is defined as [19]:

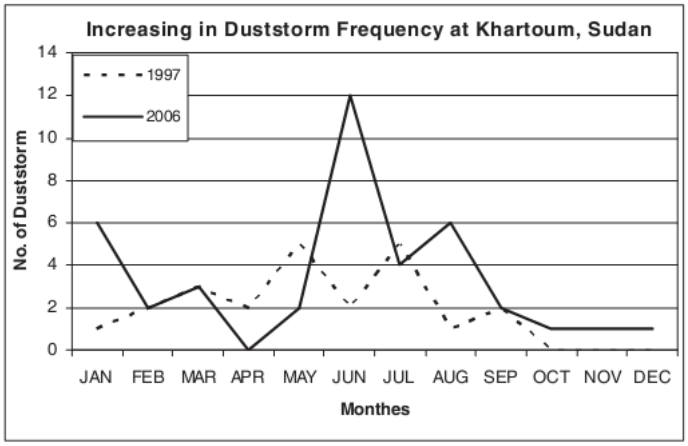

Figure 1.2: Increasing number of dust storms in Khartoum, Sudan, (1997, 2006). [18]

$$\text{Extinction} = \text{Scattering} + \text{Absorption} \tag{1.1}$$

Due to the dust particles' small radii compared to the wavelength, the attenuation of the propagating EMW in a dusty medium can be predicted using Rayleigh scattering based models together with the vertical dust particles size distribution. On the other hand, the complex Mie scattering, which is described by Mie solution to Maxwells equations, based models can be used together with the sand particles' size distribution to predict the attenuation of the propagating waves.

Visibility, or optical visibility, is an important factor in the attenuation prediction equations. The visibility, measured in metres, is directly proportional to the attenuation. A severe dust storm can reduce the visibility to few metres as seen in Figure 1.3. As the visibility decreases, the attenuation to the propagating wave will increase. This might have a serious effect on the long-distance travelling EMW, such as radar signals.

One of the serious effects of heavy dust storms is the obscuring of the satellite view as shown in Figure 1.4. This limits the ability of the satellites to observe the ground. Figure 1.4(a) shows also the ability of the dust storms to extend over large areas, from 10 to 500 km, as reported by Ansari and Evans [8], with average

Figure 1.3: Left: Marib, Yemen 2005; Right: Kuwait, Kuwait 2011. (www.tripadvisor.com, www.drillingahead.com)

duration of 3 hours [8]. Heavy dust storms prevent satellites from monitoring the sea-land borders as shown in Figure 1.4(b). The dust storm might extend from one continent to another as shown in Figure 1.4(c).

1.2 Problem Statement

All of the attenuation observation experiments were performed using communication links where the attenuation was measured in the receiving station. The validation of the available attenuation prediction models in the literature is still lacking. It is very rare that the radar applications are taken into consideration. As the radar signal travels to the target then back to the radar (two ways), it is subjected to far larger attenuation than experienced by the communication links, bearing in mind that the radar signal travels very long distances in both directions.

The increasing interest in using several radar applications, such as: guarding bor-

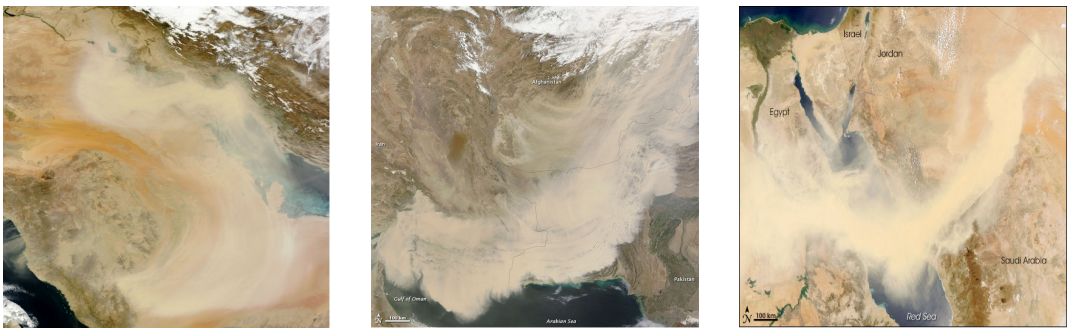

(a) Dust Storm over Saudi Arabia and the Persian Gulf, March 2012

(b) Dust Storm in Southwest Asia, March 2012

(c) Dust Storm over the Red Sea, May 2005

Figure 1.4: Sattelite images of Dust Storms (http://earthobservatory.nasa.gov).

ders, monitoring smuggling operations monitoring and observing enemy movements in wartime, in arid and semi-arid areas(which frequently encounter dust storms), increases the importance of studying the EMW behaviour, especially radar signals, when propagating in a dusty medium. Signal attenuation forms the most critical effects of the dust storm especially for radar applications and its prediction models need to be investigated.

An accurate validated attenuation model will help both radar operator and design engineers to try to compensate for this attenuation and reduce the effects of dust storms on the propagating radar signal.

1.3 Objectives

Several EMW attenuation prediction models have been developed in the past 50 years. The main goal of this study is to evaluate the performance of available models and to validate them against the few available measurements; also, to analyse the relation between the attenuation and some factors, such as visibility, dielectric constant, particles size distribution and the effect of dust storm height. The scarceness of practical experiments in this field and hence the limited number of measurements restrict accurate validation of the available models.

The objectives of this project are:

- A critical review of the electromagnetic wave propagation in dusty mediums, i.e. through dust storms.
- Compare the predictions of the mathematical attenuation models with the measurements available in the literature.
- The applicability of the signal attenuation prediction models to radar applications.

1.4 Overview

This section serves as an overview of the project report. It will also describe the approach followed to achieve the previously mentioned objectives.

Chapter II discusses the morphological and electrical properties of dusty mediums. Silt and clay are the two main constituents of the dust. The dust particles' shape in dusty mediums is random as they vary from needle-like shapes to sphere or disc shapes as reported by Sharif [4]. The dust particle shape plays a major role in deriving the EMW attenuation prediction models.

Most of the attenuation models assumed a spherical dust particle shape while deriving their attenuation models. This assumption reduces the mathematical complexity involved in finding the attenuation, specially when finding dusty mediums effective permittivity. This assumption allows the use of a well-known in-homogeneous dielectric mixture effective permittivity rule given by Patil [20], which is based on the Maxwell Garnette (MG) mixing rule. In nature, it is very rare to find the dust particle in a perfectly spheroid shape.

Assuming an ellipsoidal dust particle shape gives three degrees of freedom and forms a good approximation to the realistic dust particle shapes. Ghobrial and

Sharif [5] and Rai [10] derived complex equations for the medium dielectric permittivity which requires the calculation of the depolarisation factor along the ellipse axes.

The dust particles' radii vary between 0.1 μm to 50 μm, Sharif [4]. Xiao et al. [2] claimed that the dust particles radii can be upto less than 60 μm . The particles radii decrease as the height increases according to a vertical dust particles size distribution, hence the visibility will increase with the height. Chu [15] assumes an equisized particles size distribution which is unrealistic. Ghobrial, according to Alhaider et al. [6], and Haddah et al. [3] reported that the dust particles' vertical size distribution is best fit with an exponential distribution. Both conclusions were based on only one sample observation.

Alhaider et al. [6] tested the dust particles size distribution for 16 different samples. Fourteen out of the 16 samples were best described by log-normal and normal distributions. The remaining two samples were best fit by power low distribution. At a height of 21 m, three of five collected samples were best described by log-normal distribution and the other two can be explained by normal distribution. It becomes clear that the dust particles size distribution in dust storms may differ from one storm to another, based on the geographical location and the climatic conditions.

The difficulties involved with measuring the optical attenuation and the dust mass concentration led to the use of visibility as an alternative choice. Visibility can be used instead of optical attenuation and dust mass concentration as they are related by mathematical expressions. Chu [15] gave the relation between optical attenuation as:

$$\alpha_0 = \frac{15}{V} \tag{1.2}$$

where α_0 is the optical attenuation and V is the visibility.

Patterson and Gillette [13] derived a relation between the dust mass concentration (M) and the visibility (V) as:

$$MV^{\gamma} = C \tag{1.3}$$

where γ and C [kg/m^3] are constants that depend on the originating geographical area of the dust storm and the climatic conditions.

Another critical factor that plays a major role in the attenuation prediction of a propagating EMW in a dusty medium is the medium's dielectric constant. The moisture content of the dust has a serious effect on the value of the dielectric constant of the dust. The dielectric constant increases, and hence the attenuation changes, with the moisture content of the dust.

Chapter III starts with a review of the scattering regimes, or domains, and their applicability to microwave signals. The scattering regimes are:

$$\alpha = \begin{cases} \frac{2\pi r}{\lambda} & \ll 1 \quad \text{Rayleigh Scattering (small particle compared to wavelength of light)} \\ \frac{2\pi r}{\lambda} & \approx 1 \quad \text{Mie Scattering (particle about the same size as wavelength of light)} \\ \frac{2\pi r}{\lambda} & \gg 1 \quad \text{Geometric Scattering (particle much larger than wavelength of light)} \end{cases}$$

where α is the size parameter, r is the particle radius and λ is the wavelength.

The scattering regime that is applicable to the microwave (MW) and millimetre wave (MMW) is the Rayleigh scattering due to tiny dust particles radii compared to the propagating signal wavelength.

Several efforts have been made to come up with mathematical attenuation prediction models in the past 50 years. In 1978, Chu [15] derived the first known attenuation prediction model for microwave signal propagating through dust storm. This model was based on the Rayleigh approximations. It was assumed that the dusty medium is a mono-dispersive (equal particles radii) system and all particles in the medium were perfect spheres. After that, the Chu model has been

modified independently by Ghobrial and Sharif [5] and Goldhirsh [21] and [22]. Both modifications made use of the relation between visibility and mass concentration given by Patterson and Gillette [13] and arrive at identical mathematical formulas.

Rayleigh scattering assumptions have some inherent limitations that appear as the frequency increases. The microwave attenuation in a dusty medium depends on frequency, particle size and the dielectric constant. Vishvakarma and Rai [1] observed that at higher frequencies, higher than 40 GHz, the predicted attenuation will be associated with a large deviation. This deviation is due to the inherent limitation of Rayleigh scattering assumptions.

Due to the above-mentioned deviation, Abdulla et al. [23] suggested the use of the first three terms of the Mie extinction formula to develop an electromagnetic wave, propagating through a dusty medium, attenuation prediction model. This model was slightly modified by Islam et al. [24]. The size parameter α is much smaller than 1 for the microwave signals. As a result, the use of the Mie solution is theoretically not feasible. The use of the Mie solution to predict the attenuation for a dusty medium becomes more feasible for very high frequency ($\geq$500 GHz).

The last attenuation model presented in Chapter III is the model derived by Xiao et al. [2]. This model makes use of the effective material property technique together with the general formulation of the complex propagation factor of the dusty medium. The attenuation in this model is obtained directly from the general formulation of the wave propagation constant based on an equivalent complex permittivity of the dusty medium [2]. This model produce comparable results and performance to the Rayleigh scattering based models.

All the above attenuation prediction models were based on the assumption of spherical dust particles. A more realistic assumption concerning dust particle shape is ellipsoid. This assumption provides three degrees of freedom and gives a more realistic approximation to real dust particles as it covers a wide variety of shapes by changing the ellipsoid axes ratios.

Ghobrial and Sharif [5], Dong et al. [25] and Rai [10] developed mathematical

attenuation models under the assumption of ellipsoidal dust particles. These models are claimed to give a more accurate prediction compared to the models that are based on the assumption of spherical dust particles. This claim has not been verified practically. The only disadvantage of these models is their mathematical complexity as they require the evaluation of depolarisation factors along each of the ellipsoid axes.

The chapter ends with a performance analysis of the models where the results of each model is compared with the available measurements and with that of the other models. This performance test is implemented in MATLAB.

Chapter IV discusses the effect of the charged dust particles on the attenuation. As the wind blows the sand and dust particles during a storm, the particles gain some charge, Zheng et al. [26]. The interaction between the wind and the dust particles and the collision and the friction between particles form the main causes of charging the particles. Experiments and observations, discussed by Zheng et al. [26], of the electric field have confirmed the existence of the charges on the dust and sand particles. According to Zheng et al. [26], some observations showed the decrease in the particles charge with increasing the measurement height.

The charge will be distributed only on the top cap of the sand and dust particles [26]. The amount of the charge on the particle has a direct relationship with the amount of the attenuation that occurs to the propagating electromagnetic wave through dusty mediums. Zhou et al. [11] showed that the charged sand/dust particles attenuate the signal more than the uncharged particles.

If the particle charge is distributed uniformly on the particle surface, then the attenuation caused by this particle will be as if the particle has zero charge (uncharged particle) [11]. In the case of the uncharged particles, the attenuation occurring to the propagating wave can be found by the attenuation models presented in Chapter III.

The final chapter, Chapter V, concludes that the assumption of perfect spherical dust particles, which simplify the attenuation calculation, in the dust storm is not accurate as the particles have random shapes. Assuming all dust particles

in a dust storm are ellipsoid with different axes ratios will provide three degrees of freedom and give better and realistic approximation to the dust particles in nature. In addition, it will increase the complexity of the attenuation prediction mathematical models as it requires the calculation of the depolarisation factors along ellipsoidal particle axes.

The Rayleigh scattering based attenuation prediction models suffer from large deviation from the measurements as the frequency of the propagating EMW increases. Several reasons may contribute in this behaviour, such as the invalid dust particles geometry, as they assume perfect spheroid particles, and the increase of the particles scattering cross-section contribution to the extinction cross section.

The attenuation prediction models that make use of the effective material property technique have a similar performance to the Rayleigh-based models. Also, it suffers from large errors as the wave frequency increases.

The use of the Mie solution to derive an attenuation prediction model is theoretically invalid as the size parameter α, ratio of particle radius to the propagating signal wavelength, is much smaller than one. This model is inconsistent with the Mie theory and might be fortuitous. By using the constants given by Kerr [27] in the attenuation prediction model that utilises the Mie solution, the model gives identical attenuation predictions of the model derived by Chu [15], which is based on Rayleigh approximation.

The existence of charges on the particles' surface will increase the attenuation caused by the particles. The attenuation due to charged sand and dust particles depends on two additional factors: the amount of the charge on the particle and the charge distribution angle on the particle. These factors are difficult, and might even be impossible, to measure which has led to the neglect of the dust particles' charge effect.

According to Zheng et al. [26], the dust particle possesses negative charges. This charge has less effect on the overall wave attenuation. The particles' charges become more negative as the measurement height increases. This reduces the

effects of the charges on the dust particles on the overall attenuation of the wave propagating through dusty mediums.

Chapter 2

Morphological and Electrical Properties of Dusty Mediums

This chapter serves as a review of the morphological and electrical properties of a dusty medium as they form the two main contributors to the attenuation of the EMW propagating in this medium. Understanding of both properties is an essential part of the process of studying and evaluation the attenuating prediction models.

The geometry of the dust particle is an important factor to be investigated as it gives an idea of the behaviour of the incident wave when interacting with the dust particle. Another factor that will have an effect on this interaction is how the dust particles are aligned in a dust storm.

The dust particle sizes decrease with the measurement height. The relation between the measurement height and the dust particle sizes is investigated and the vertical distribution of the dust particle sizes is discussed.

Visibility and dust dielectric constant are the investigated electrical properties of the dusty medium that have made an essential contribution to predicting the propagating wave attenuation.

2.1 Morphological Properties of Dust Particles

2.1.1 Geometry

Shape and Alignment

The shapes of the dust particles are completely random irregular with no particular symmetry. Sharif [4] looked at various dust particles under the microscope and concluded that the their geometry cannot be explained by one simple geometry; rather they have various and sometimes complicated geometries. The shapes varied from needle-like to discs or spheres [4].

Most of the attenuation prediction models in the literature for an EMW propagating in a dusty medium assume the dust particle shapes as perfect spheroids. This assumption leads to more mathematical simplifications when predicting the attenuation as the particles' radii will be the only variable.

A more realistic assumption is to assume dust particles to have ellipsoidal shapes as shown in Figure 2.1. This assumption is a good approximation to realistic dust particles as the ellipsoid has three degrees of freedom. By varying the ellipse axes ratios, totally different shapes will result.

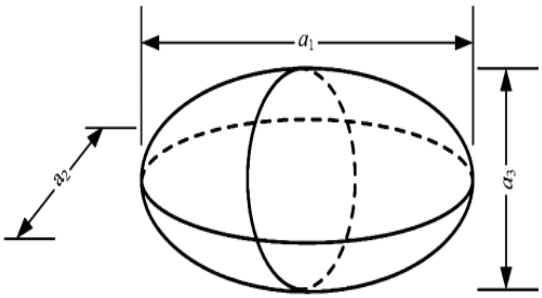

Figure 2.1: Dust particle ellipsoidal geometry approximation.

The only problem with assuming dust particles to have ellipsoidal shapes is that it increases the mathematical complexity when predicting the attenuation. The calculation of the medium effective dielectric constant involves evaluation of integrals to find the depolarisation factors along each axis of the ellipse.

Different alignments of the spherical dust particles in a dust storm does not make any difference as all points on the particle surface will have the same distance from the particle centre. In case of the ellipsoidal shape assumption, the ellipsoidal shapes are oriented with shortest axis vertical and the other two axes are randomly oriented if there is no air flow. Because of air flow turbulence as the wind blows, the ellipsoidal dust particles will be randomly oriented.

Size

Silt and clay are the two main constituents of the dust. In the mathematical attenuation prediction models available in the literature, both silt and clay are assumed to have spherical shapes. The silt particles have radii that fall in the range between 2 μm to 50 μm. The clay particles have radii that are less than 2μm. Haddad et al. [3] reported that more than 30% of the particles in a dust storm have radii of less than 5 μm. Table 2.1 shows a natural dust sample, collected at height of 3 m above the ground by Haddad et al. [3], different particle sizes with different weight ratios reported by [3]. Figure 2.2 shows that as the particles get smaller, their cumulative weight in a dust storm will be larger. It has been found out that the sample contains sand, silt and clay. The existence of sand particles might be due to low measurement height.

Table 2.1: Natural dust sample, collected during dust storm, particles sizes and percentage of weight. [3]

Radius (μm)	Weight (%)	Cumulative (%)
250	1.04	1.714
125	2.3	5.504
62.5	5.585	14.708
15.5	23.25	53.026
7.8	16.5	80.22
3.9	8	93.403
1	4	99.996

Sharif [4] reported that dust particle radii vary from 0.1 μm to 42 μm. Alhaider et al. [28] found that the dust particle radii vary between 10.5 μm to 21.25 μm when measured at a height of 1 metre, and at a height of 21 metres, the radii range

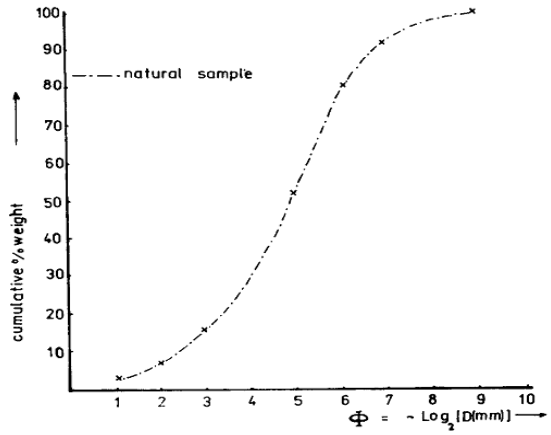

Figure 2.2: Cumulative percentage weight vs $\phi = -\log_2(D_{mm})$ curves of the natural dust sample. [3]

between 8 μm and 9.2 μm. Ansari and Evan [8] reported that: dust particles with radii of less than 5 μm constitute more than 30% of the total population of the dust storm.

The sizes discussed above are measured under the assumption that all dust particles have spherical shapes. If the dust particles are assumed to have ellipsoidal shapes, further measurements are required to find the ratios of ellipse axes, indicated in Figure 2.1. Ghobrial and Sharif [5] measured the ellipsoid axes ratios for over 500 sand/dust particles. The ratios (a_1/a_2 and a_2/a_1) probability density functions are shown in Figures 2.3 and 2.4 and are best fit with normal distribution with a variance of 2 [4]. The right-hand parts of the two figures give the probability of finding the axial ratio in the specified interval [5]. The average ratios and the standard deviations are found to be:

$$r_1 = a_3/a_2 = 0.75; \quad std = 0.70 \tag{2.1a}$$

$$r_2 = a_2/a_1 = 0.71; \quad std = 0.64 \tag{2.1b}$$

$$a_1 : a_2 : a_3 = 1 : 0.71 : 0.53 \tag{2.1c}$$

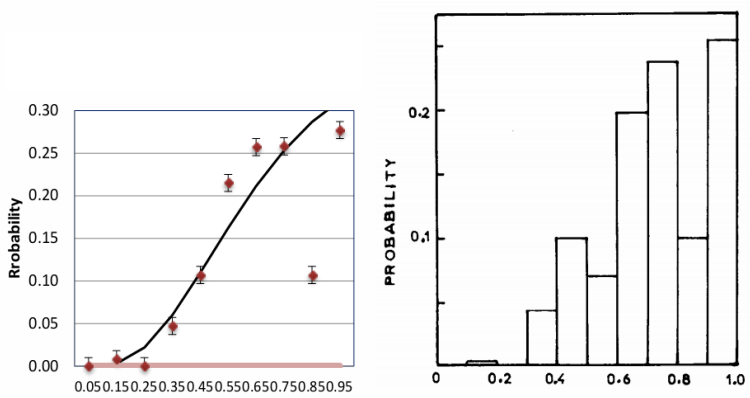

Figure 2.3: Axial ratio $r_1 = a_3/a_2$. [4], [5].

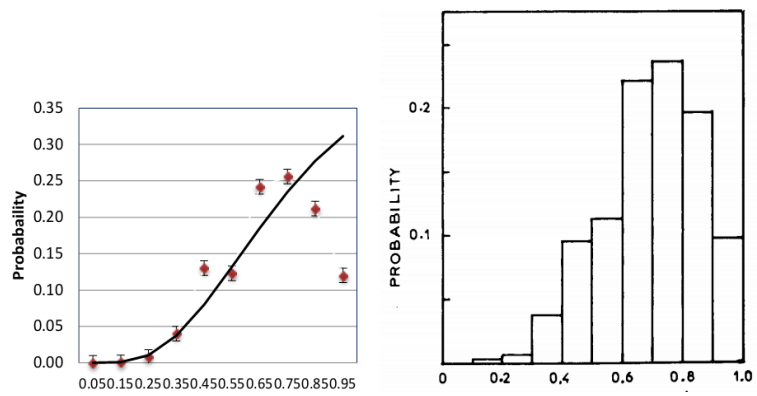

Figure 2.4: Axial ratio $r_2 = a_2/a_1$. [4], [5].

2.1.2 Particles Radii Variation With Height

As the measurement height increases, the dust particles will get smaller and hence the attenuation. Alhaider et al. [6] came up with an empirical formulas that describe the relation between both average and effective particle radii and the height. Figure 2.5 shows that the variation of particle radii with the height is best described by power low as follows [6]:

$$r_{avg} = r_{0a}[h/h_0]^{-\gamma_a} \quad ; \qquad \gamma_a = 0.15 \tag{2.2a}$$

$$r_e = r_{0e}[h/h_0]^{-\gamma_e} \quad ; \qquad \gamma_e = 0.04 \tag{2.2b}$$

where r and r_0 are the particles radii at heights h and h_0 respectively.

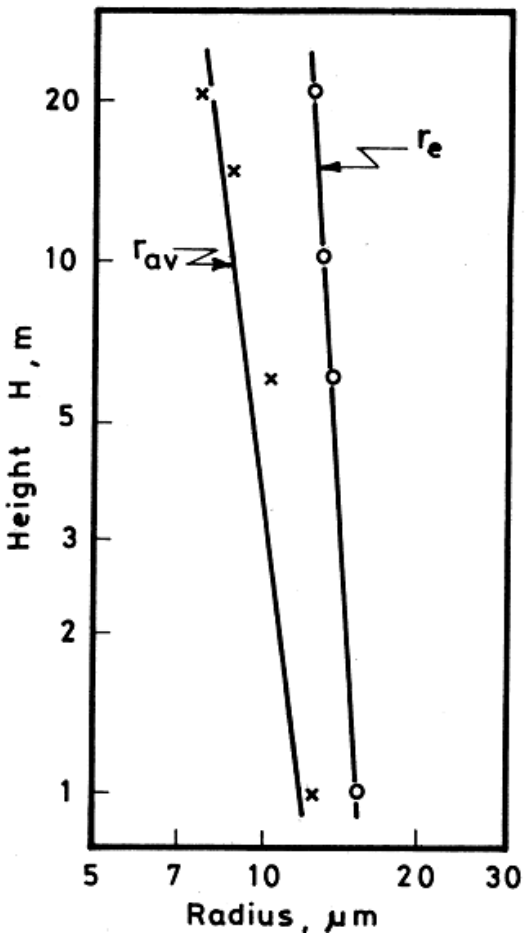

Figure 2.5: Particles effective and average radii, r_e and r_{av}, variation with height. [6]

2.1.3 Dust Particles Size Distribution

As mentioned before, the particles' sizes change with height -become smaller as height increases. Several efforts were made to study the particles' vertical size distribution. In 1979, Chu [15] assumed the particle radii in a dust storm to be between 10 μm and 100 μm. Further, he assumed that the dust particles in a dust storm to have equisized distribution [6] which is an unrealistic assumption.

Ansari and Evans [8], 1982, reported that Ghobrial carried out experiments to analye the dust particles size distribution in Sudan. This study reveals that the

dust particles' size distribution follow an exponential distribution of the type:

$$P(r) = \beta exp(-\beta r) \tag{2.3}$$

with a to have a mean value of $\overline{a} = 1/\beta$

In 1983, Haddad et al. [3] found that the particles' size distribution is best fit by an exponential distribution function. The decision was made based only on one collected dust sample, collected from real dust storm, that is collected at a height of 3 metres above the ground level and using the pipette method for sample analysis. Figure 2.6 shows the particles' size distribution found by [3].

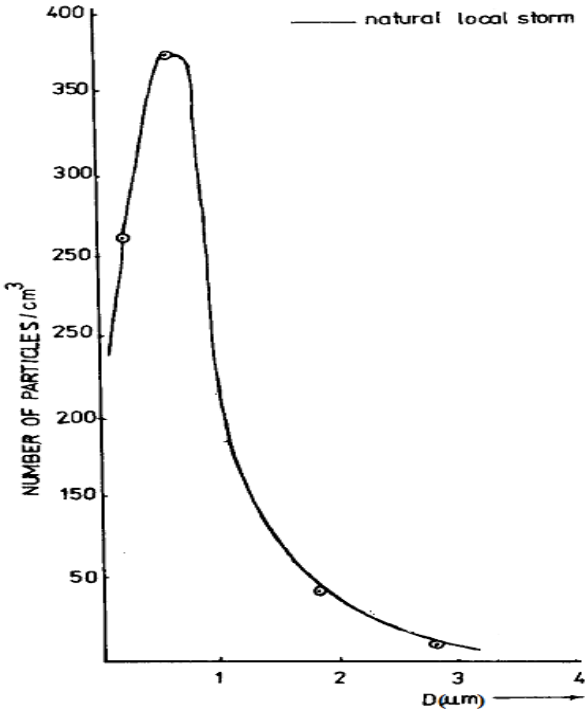

Figure 2.6: Dust particles size distribution in a dust storm. [3]

Rowe et al. [29], 1985, performed an experiment on the indoor-outdoor relationship of suspended particulate matter at the engineering laboratories, King Saud University, Riyadh, Saudi Arabia. This study concludes that of the air-suspended particles, size less than 10 μm, size distribution is best described by normal distribution.

In 1987, Sharif [7] utilised both hydrometer and pipette methods to analyse size distribution of sand and dust particles. In this experiment, twelve sand/dust samples were collected in two different cities, 300 km away from each other, in Sudan between 1981 and 1983. The samples were collected at ground level.

The collection of samples at ground level led to the inclusion of large particles, sand particles that cannot be elevated to more than a few metres, typically 2-5 m. The inclusion of sand particles may have negative effects on the study of the dust particles size distributions.

The study reveals that the cumulative dust particles size distribution is best fit by a straight line. The average probabilities of different particles sizes for the collected samples are shown in Table 2.2. Figure 2.7 shows the curves of the cumulative particles size distribution of five different samples. The straight line equation can be given by [7]:

$$F(W) = a + bD \tag{2.4}$$

where $F(W)$ is the weight fraction occupied by particles having a diameter of less than D (μm).

The constants a and b, which depend on the distribution characterising factor, values are estimated using least square method. The value of a ranges between -0.3551 and 0.046 with average value of 0.0144, and the constant b value ranges between 0.0055 and 0.0098 with average value of 0.0072. [4]

In 1987, Alhaider et al. [6] performed tests on dust particles size distribution on 16 different dust samples that are collected at five different heights and from five different dust storms in Riyadh, Saudi Arabia between 1985 and 1986. The sample heights are indicated in Figures 2.8 and 2.9. Passive collectors were used to collect the dust samples as they have the advantage of being able to collect wide ranges of dust particles sizes [6]. The samples' preparation method is explained in great detail in [6]. The meteorological parameters of the five dust storms are shown in Table 2.3.

Table 2.2: Average probabilities of different particles sizes in 12 different dust storms samples. [7]

Particle Diameter (μm)	Probability
300.0 - 100.0	0.012
100.0 - 50.0	0.232
50.0 - 10.0	0.404
10.0 - 5.0	0.091
5.0 - 1.0	0.141
1.0 - 0.5	0.060
0.5 - 0.1	0.062

The samples were collected at four different heights as shown in Table 2.4. It is clear from the table that both effective and average particle radii decrease as the height increases and hence the attenuation decreases. The particles' size distribution type varies between normal, log-normal and power low.

Using the 'least squares fitting' method, it was found that 14 of these samples are best described by normal and log-normal functions while the other two samples are best described by power low as indicated in both Figures 2.8 and 2.9. For a measurement height of 21 m, the distribution is either normal or log-normal. In conclusion, the geographical location, soil properties and wind speed are important factors involved in shaping the particles size distribution.

In 1988, Abdulla et al. [23], performed a study on the dust particles size distributions over several dust samples collected in 1985 from several dust storms at a height of 20 m in the city of Baghdad, Iraq. Five different techniques were used to complete this study, namely: hydrometer, pipette, sedimentation balance, optical microscope and Coulter counter. The detailed experiment procedure can be found in [23].

This study revealed that almost identical results were achieved from different techniques used for all the tested samples. It was found that the cumulative dust particles distribution can be well be described by log-normal and a third degree polynomial functions for sand/dust particles with radii range from 1 μm to 100 μm.

Table 2.3: Meteorological Parameter of Five Dust Storms In Riyadh, Saudi Arabia. [6]

Storm Event	Date and Time (Local Time)	Meteorological Parameters				
		Wind Speed (m/s)	Pressure (mb)	Temp. (°C)	Relative Humidity (%)	Visibility (km)
I	23.3.85 (19-01)	18.0	956	29	90	1.6 - 2.0
II	22.4.85 (15-15:30)	16.5	956	28	70	1.6 - 2.0
III	23.4.85 (16-18)	8.2	956	36	80	5.0 - 6.0
IV	09.2.86 (17-18)	18.0	948	19	88	3.0 - 4.0
V	25.3.86 (18:50-23)	20.6	943	32	37	0.6 - 1.0

Table 2.4: Dust particles size distribution for 16 dust samples collected from five different dust storms at different heights. [6]

Dust storm Event-sample number	Height (m)	Average Radius (μm)	Effective Radius (μm)	Probability density function	% decrease in attenuation with height
I - 1	21	9.2	15.45	Log-normal	34%
I - 2	15	9.8	19.90	Normal	15%
I - 3	1	14.0	24.0	Log-normal	-
II - 4	21	8.50	13.20	Normal	53%
II - 5	15	9.0	15.70	Power low	44%
II - 6	1	18.5	28.0	Power low	-
III - 7	21	8.0	11.40	Normal	31%
III - 8	15	8.5	15.50	Log-normal	11%
III - 9	1	10.5	16.30	Log-normal	-
IV - 10	21	7.20	10.0	Log-normal	19%
IV - 11	15	7.50	11.80	Normal	15%
IV - 12	6	8.50	12.30	Normal	-%
V - 13	21	8.30	13.0	Log-normal	51%
V - 14	15	9.20	14.60	Log-normal	45%
V - 15	6	15.30	19.80	Log-normal	26%
V - 16	1	21.30	26.80	Normal	-%

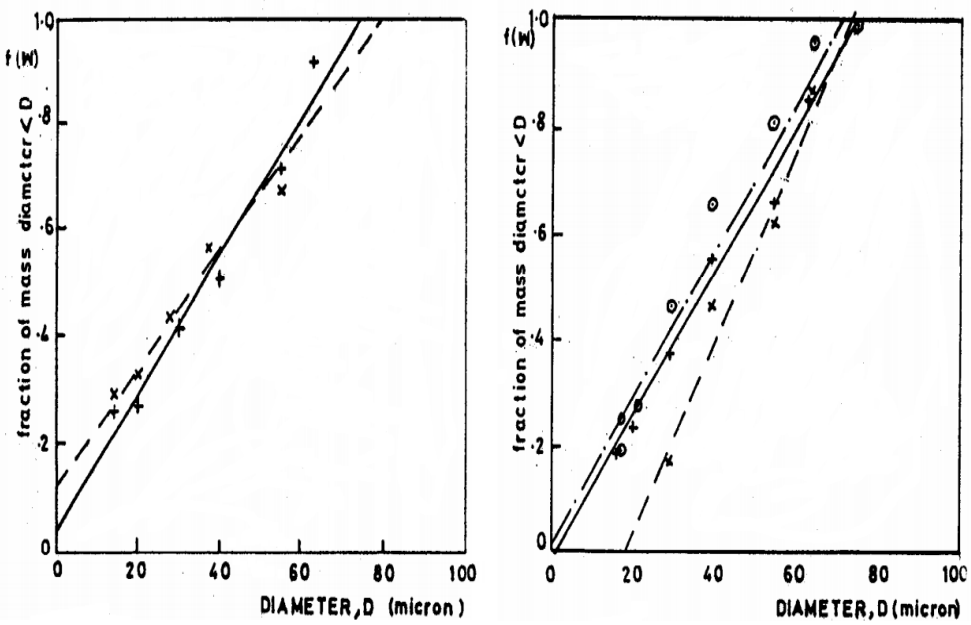

Figure 2.7: Dust particles size distribution in a dust storm. [7]

Sviridenkov et al. [30], 1989, performed a study of the aerosol particles size distributions during the Soviet-American experiment in Tadzhikistan. The conclusion of this study was: the arid aerosol particles, with diameters between 3.5 μm and 6 μm, size distribution can be approximated by log-normal distribution with σ^2 = 0.5 to 0.8.

As can be noticed, the distribution functions differ from one study to the other. In Alhaider et al. [6] study, different samples that are collected from the same dust storm at different heights have different distribution functions. This indicates that the distribution functions vary with the measurement height. Particle size dependence on both geographical location and storm parameters, mainly its speed, may provide a good explanation of the results inconsistency.

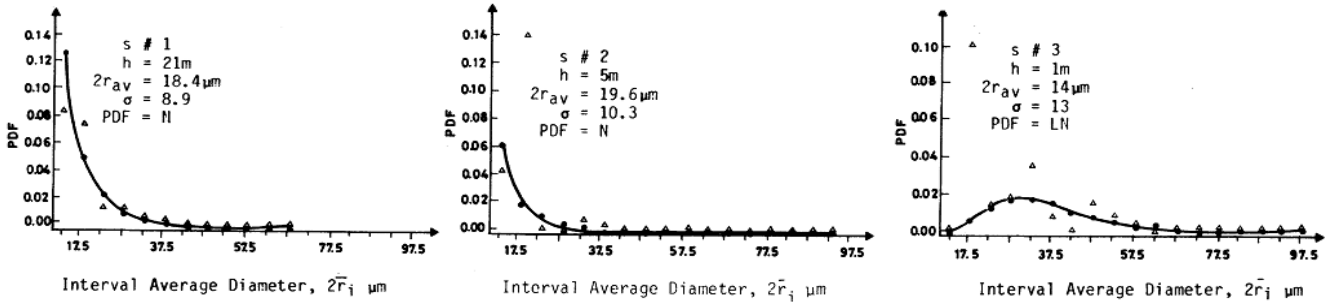

(a) Dust storm I, Visibility = 1.6 - 2.0 km.

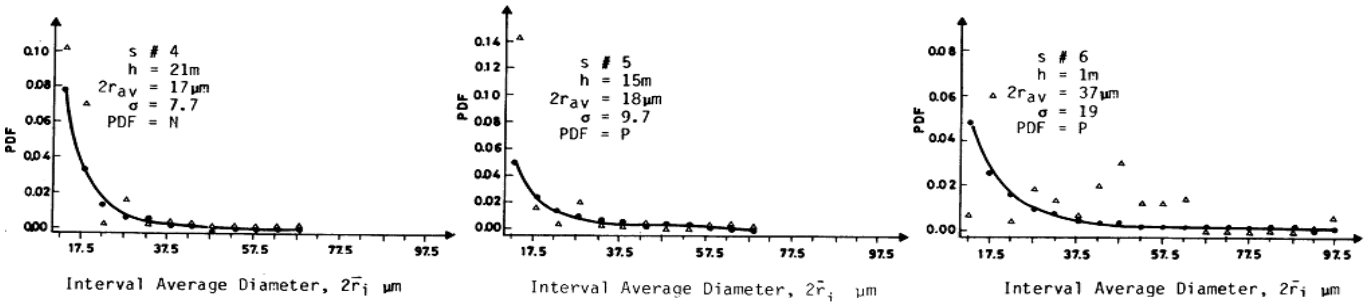

(b) Dust Storm II, Visibility = 1.6 - 2.0 km.

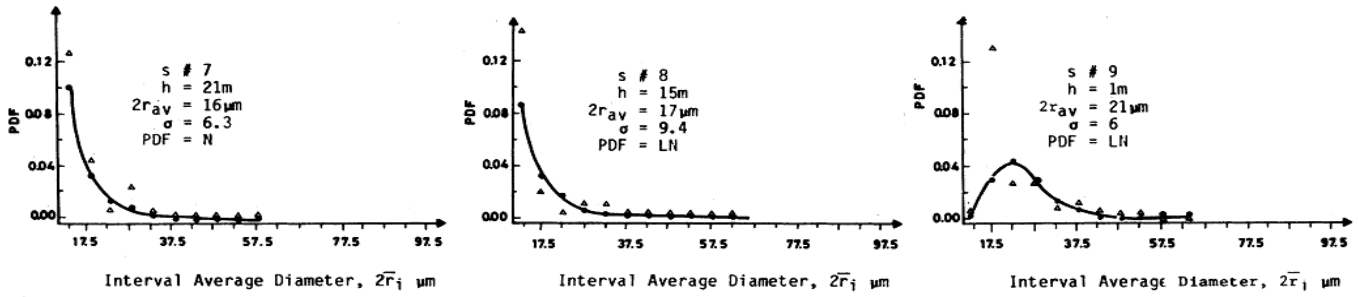

(c) Dust Storm III, Visibility = 5.0 - 6.0 km.

Figure 2.8: Particles size distributions at different measurements heights for dust storms I, II and III. $s\#$: sample number; h: height; σ: standard deviation; PDF: probability density function; r_{av}: average particle radius; r_i radius of index i; N: Normal; LN: Log-normal; P: Power low; Δ: measured data; $\bullet$: fitted data. [6]

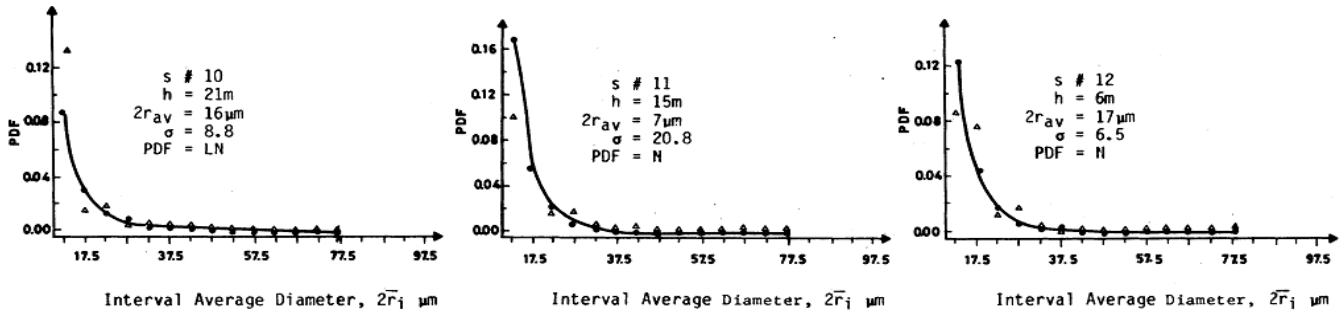

(a) Dust Storm IV, Visibility = 3.0 - 4.0 km.

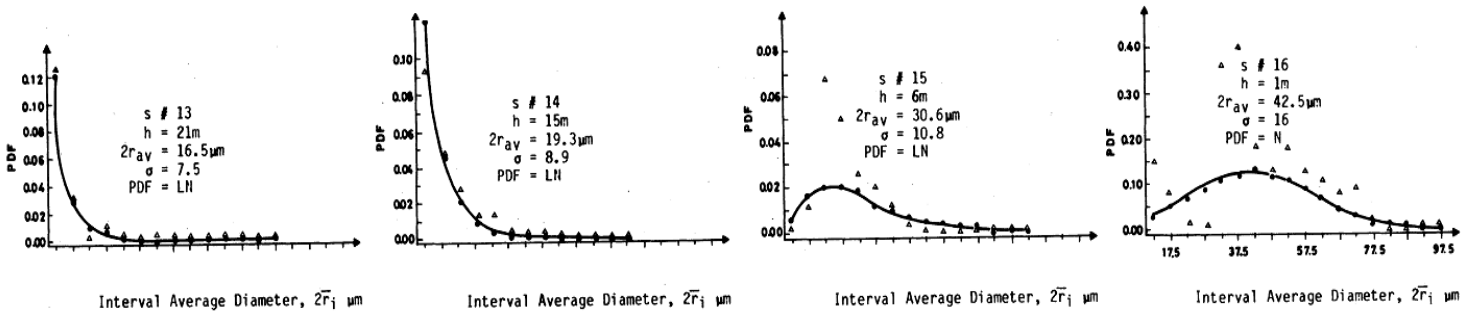

(b) Dust Storm V, Visibility = 0.6 - 1.0 km.

Figure 2.9: Particles size distributions at different measurements heights for dust storms IV and V. $s\#$: sample number; h: height; σ: standard deviation; PDF: probability density function; r_{av}: average particle radius; r_i radius of index i; N: Normal; LN: Log-normal; P: Power low; Δ: measured data; $\bullet$: fitted data. [6]

2.2 Dust Electrical Properties

2.2.1 Visibility in dust storm

Visibility or optical visibility forms a critical factor in the attenuation prediction calculations. The attenuation that occurs on a propagating EMW through dust storms increases as the visibility decreases. Long-time duration of low-visibility dust storms will have more impact on the propagating wave, especially the attenuation. Tables 2.5 and 2.6 provide an idea of the dust storms' period of stay in two cities in Saudi Arabia and five different locations in Sudan. As the dust storms last for a longer time, their effects on the propagating signals will be enhanced.

Table 2.5: Visibility average time per year based on 15 years record at Jeddah and Riaydh, Saudi Arabia. [12]

	Average No. of minutes/year	
Visibility (m)	Jeddah	Riyadh
10	78	24
100	175	690
200	275	870
300	340	1272
400	385	1502
500	480	2332

Visibility vs Mass Concentration

Patterson and Gillette [13] studied the relation between the visibility and the particles' mass concentration to determine the particulate concentration in the atmosphere. This relation provides provide another mean of finding the visibility from the particles mass concentration and vice versa.

If M is the particulate mass concentration, V is the visibility and C is a constant, the relation between the mass concentration and the visibility can be given by [13]:

$$MV = C \tag{2.5}$$

The constant C varies with different particles size distributions. Using empirical data, the relation can be modified to [13]:

$$MV^{\gamma} = C \tag{2.6}$$

where γ is another constant. The constant C and γ depend on the dust storm's originating geographical area, soil type and the climatic conditions [13].

In 1973 and 1974, Patterson and Gillette [13] made 13 observations, at 2 m measurement height, during several dust storms with visibilities of less than 11 km as shown in Table 2.7.

The constant C is calculated for three different cases:

- Total mass C^{tot}.
- Small particles mode; radius: $r < 10\mu$m.
- Particles with radii $< 20\mu$m.

For the total mass, C^{tot} ranged between 9×10^{-3} and 3.9×10^{-2} [g.km/m^3], with a mean value $C^{tot}_{mean} = 0.023 \pm 0.004$ [g.km/m^3]. The individual values of mass concentration M and visibility V are used to find C using Equation 2.6. The results are shown in Table 2.8.

In case of local erosion, the constant C values range between 2.0×10^{-2} and 1.0×10^{-1} [g.km/m^3]. In this case the value of C will depend on wind speed, soil conditions and visibility. If there is no local erosion in the dust storm source region and the storm is still in the dust generation region, the convenient value of C is 2.0×10^{-3} [g.km/m^3]. If the tested area is several thousand kilometres from the dust source, the 1.4×10^{-3} [g.km/m^3] is the appropriate value for C. [13]

Table 2.6: Visibility statistics in between 1975 and 1980 in Sudan. [4]

	Hours/Annum			
Visibility (m)	Khartoum	AbuHamad	Elobied	Atbara
0-100	3.80	0.61	2.37	0.79
100-200	5.40	4.82	4.03	1.59
200-300	6.13	4.03	6.22	1.60
300-400	7.27	7.53	3.77	6.18
400-500	6.75	2.45	4.20	3.85
500-600	8.41	15.16	4.56	6.75
600-700	3.77	19.62	2.63	8.76
700-800	2.63	6.83	0.35	10.16
800-900	21.64	17.34	13.67	17.43
900-1000	0.79	9.11	1.40	4.38

Table 2.7: Visibility and mass concentration obsevations, USA, TX. [13]

Date	Location	Wind Speed [mph]	Visibility [km]	Mass Concentration [g/m^3]
3.4.1973	Bronco, TX	28	0.26	1.4×10^{-1}
4.4.1973	Bronco, TX	20	3.2	5.2×10^{-1}
4.4.1973	Bronco, TX	22	1.0	2.1×10^{-3}
17.4.1973	Union, TX	30	0.20	8.1×10^{-2}
19.4.1973	Union, TX	28	0.20	1.1×10^{-2}
19.4.1973	Union, TX	27	0.40	9.6×10^{-1}
28.3.1974	Plains, TX	28	0.92	1.0×10^{-2}
30.3.1974	Plains, TX	18	8.0	2.0×10^{-2}
31.3.1974	Plains, TX	32	0.47	6.9×10^{-3}
31.3.1974	Plains, TX	28	0.69	2.0×10^{-2}
31.3.1974	Plains, TX	24	1.6	1.7×10^{-2}
2.4.1974	Plains, TX	39	0.06	4.4×10^{-1}
2.4.1974	Plains, TX	38	0.06	2.5×10^{-1}

Table 2.8: Constants C and γ calculated values. [13]

	Total mass	Small particles	Particles with $r < 20\mu$m
Mean Value of C [g.km/m^3]	0.023 ± 0.004	0.013 ± 0.005	0.017 ± 0.006
Best fit value for C [g.km/m^3]	0.020 ± 0.004	0.011 ± 0.002	0.013 ± 0.003
Best fit value for γ	1.07 ± 0.009	0.95 ± 0.12	1.08 ± 0.14

Visibility Variation With Height

From previous section, the visibility can be given by:

$$V = (C/M)^{1/\gamma} \tag{2.7}$$

The dust mass concentration at different altitude as given by Ghobrial [31] can be given by:

$$M = M' \exp(-ah) \tag{2.8}$$

where M' is the mass concentration at ground level, h is the altitude in kilometres and a is a constant. Ghobrial [31] used the value of 1.35 for a as it its value vary between 1.5 for dense dust storm to 1.2 for less dense dust storm. Ghobrial [31] gave the relation between height and visibility to be:

$$V = V' \exp(bh) \tag{2.9}$$

where V' is the visibility at ground level and $b = 1.26$.

Sharif [32] use the following relation between the dust mass concentration M, in [kg/m^3], and the height h in metres:

$$M = a/h^b \tag{2.10}$$

where a and b are constants and depend on dust particles size distribution, geographical and climatic conditions. Ghobrial and Sharif [5] believed that constant C value for Sudan is 2.3×10^{-5} [kg.km/m^{-3}] and the value of the constant γ is 1.07 for Sudan. Using these values and Equations 2.6 and 2.10, Sharif [32] derived the relation between visibility and height which is given by:

$$V^{\gamma} = C[\frac{h^{b}}{a}] \tag{2.11}$$

Assuming V_0 is the visibility at reference height h_0, the relation can be written as [32]:

$$V = V_0[h/h_0]^{b/\gamma} \tag{2.12}$$

where the average value of b is 0.28.

2.2.2 Dust Dielectric Constant

The dielectric constant, or the relative permittivity, (ε) reflects the strength of the electrostatic field produced in different materials by a fixed potential relative to that produced in vacuum under similar conditions' [33]. The understanding of the dusty medium, dust storm, dielectric properties is essential to investigate the medium effects on the microwave signal propagating through. The complex dielectric constant forms the main dielectric properties of the dusty medium. It is an important component in the attenuation prediction mathematical models. This shows the importance of the knowledge of this parameter.

Several experiments in the literature were performed to measure the dust complex dielectric constant. Some of the achieved results are summarised in Table 2.9. All the experiments presented were performed on different dust samples not on dusty mediums. As can be noticed, there is inconsistency between measured values in different experiments.

Table 2.9: Measured dielectric constant of dust for different frequencies and different moisture content.

Author	Frequency (GHz)	Soil type	Moisture content $\%H_2O$	Dielectric constant $\varepsilon = \varepsilon' - j\varepsilon''$
Ansari and Evans [8]	3	Clay	0%	$2.27 - j0.0341$
	3	Clay	20.09%	$11.30 - j2.825$
Bashir and McEwan [34]	8.6	Dust(1^{st} sample)	0%	$4.90 - j0.130$
	8.6	Dust(1^{st} sample)	3%	$6.10 - j0.520$
	8.6	Dust(3^{rd} sample)	0%	$4.52 - j0.105$
	8.6	Dust(3^{rd} sample)	3%	$5.03 - j0.382$
Haddad et al. [3]	9.35	Dust	0%	$1.80 - j0.170$
	9.35	Dust	3%	$1.91 - j0.354$
	9.35	Dust	5%	$2.08 - j0.402$
	9.35	Dust	7%	$2.40 - j0.493$
	9.35	Dust	10%	$2.63 - j0.734$
Ghobrial [35]	9.4	Dust	2.4%	$4.29 - j0.229$
	9.4	Dust	3.41%	$4.38 - j0.224$
800-900	9.4	Dust	4.3%	$4.58 - j0.378$
Ansari and Evans [8]	10	loamy	0%	$2.44 - j0.003$
	10	loamy	13.73%	$13.8 - j2.484$
Bashir and McEwan [34]	10	Dust	?	$5.10 - j0.24$
	10	Dust	?	$4.48 - j0.180$

Continued on next page

Table 2.9 – *cont...*

Author	Frequency (GHz)	Soil type	Moisture content $\%H_2O$	Dielectric constant $\varepsilon = \varepsilon' - j\varepsilon''$
Bashir and McEwan [34]	10	Dust	?	$2.50 - j0.072$
	10	Dust	?	$5.33 - j0.285$
	X-band	Dust	?	$5.34 - j0.185$
	X-band	Dust	?	$5.66 - j0.325$
Ruike et al. [36]	14	Dust	?	$5.50 - j1.3$
Ansari and Evans [8]	19.35	Silty clay	3%	$3.40 - j0.200$
	19.35	Loam	12%	$4.70 - j1.1$
	19.35	Loam	22%	$13.6 - j6.80$
	19.35	Loam	30%	$16.25 - j9.25$
Ruike et al. [36]	24	Dust	?	$5.10 - j1.40$
Ansari and Evans [8]	37	Sandy clay	0%	$2.515 - j0.07353$
	37	Loam	5%	$2.88 - j0.3529$
	37	Loam	10%	$3.29 - j0.728$
	37	Loam	15%	$7.088 - j3.50$
	37	Loam	20%	$8.588 - j4.765$
Alhaider et al. [6]	37	Dust	$> 5\%$	$2.807 - j0.200$
	37	Dust	$> 10\%$	$3.00 - j0.400$
	37	Dust	$> 10\%$	$3.00 - j0.400$
	37	Dust	$> 10\%$	$3.20 - j0.800$

Continued on next page

Table 2.9 – *cont...*

Author	Frequency (GHz)	Soil type	Moisture content $\%H_2O$	Dielectric constant $\varepsilon = \varepsilon' - j\varepsilon''$
Alhaider et al. [6]	37	Dust	10%	$3.20 - j0.800$
Ruike et al. [36]	100	Dust	?	$3.5 - j1.64$

According to Ansari and Evans [8], there is a little change in both real and imaginary parts of the complex dielectric constant with the frequency for dry dust case as shown in Figure 2.10.

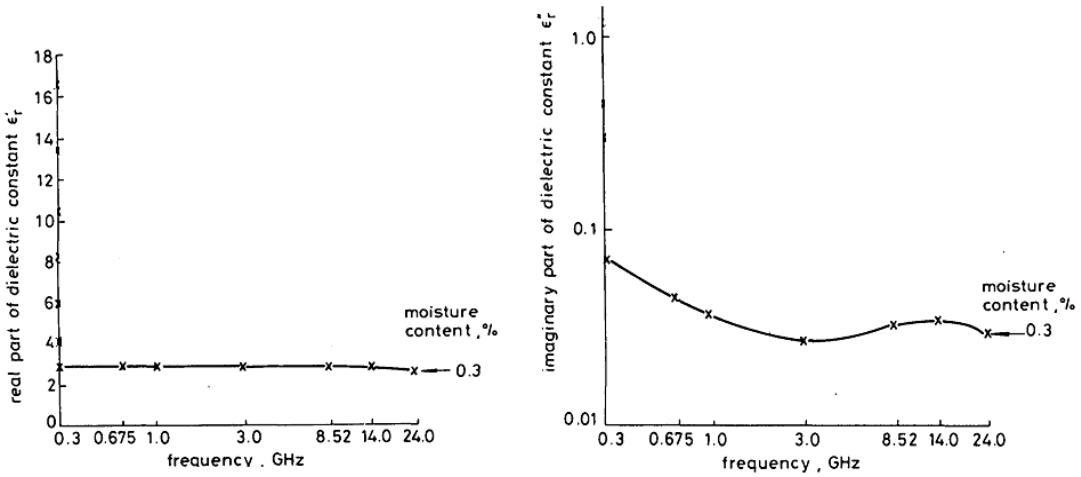

Figure 2.10: Measurement of real and imaginary parts of the complex dielectric constant of dry dust(0.3%) as a function of frequency. [8]

As mentioned above, all the measurements were done on dust samples in the lab not for dusty mediums. All the attenuation prediction models, discussed in Chapter III, use the dust samples' dielectric constant measurements to find the attenuation. As the dusty medium is far from being a solid material and the dust particles are assumed to have spherical shapes, Xiao et al. [2] uses the Maxwell Garnett mixing rule given by [20] to find the dielectric constant of the air-dust mixture. The Maxwell Garnett mixing rule is given by:

$$\begin{aligned} \varepsilon_{eq} &= \varepsilon_{air} + \frac{3v\ \varepsilon_{air}\ \left(\frac{\varepsilon_{sd}-\varepsilon_{air}}{\varepsilon_{sd}+2\varepsilon_{air}}\right)}{1-v\ \left(\frac{\varepsilon_{sd}-\varepsilon_{air}}{\varepsilon_{sd}+2\varepsilon_{air}}\right)} \\ &= \varepsilon'_{eq} - j\varepsilon''_{eq} \end{aligned} \tag{2.13}$$

where ε_{eq} is the equivalent complex relative permittivity, ε_{air} is the air relative dielectric constant and v is the volume fraction occupied by dust in a storm per unit volume. ε_{sd} is the complex relative permittivity of the dust. ε'_{eq} and ε''_{eq} are the real and imaginary parts of the equivalent complex relative permittivity.

Effect of Moisture Content and Frequency

It can be observed from Table 2.9 that the complex dielectric constant vary significantly with dust sample moisture content (or relative humidity). Ansari and Evans [8] reported that in the presence of moisture in the dust sample, the dielectric constant becomes frequency-dependent and both real and imaginary parts of the complex dielectric constant vary significantly, as shown in Figure 2.11.

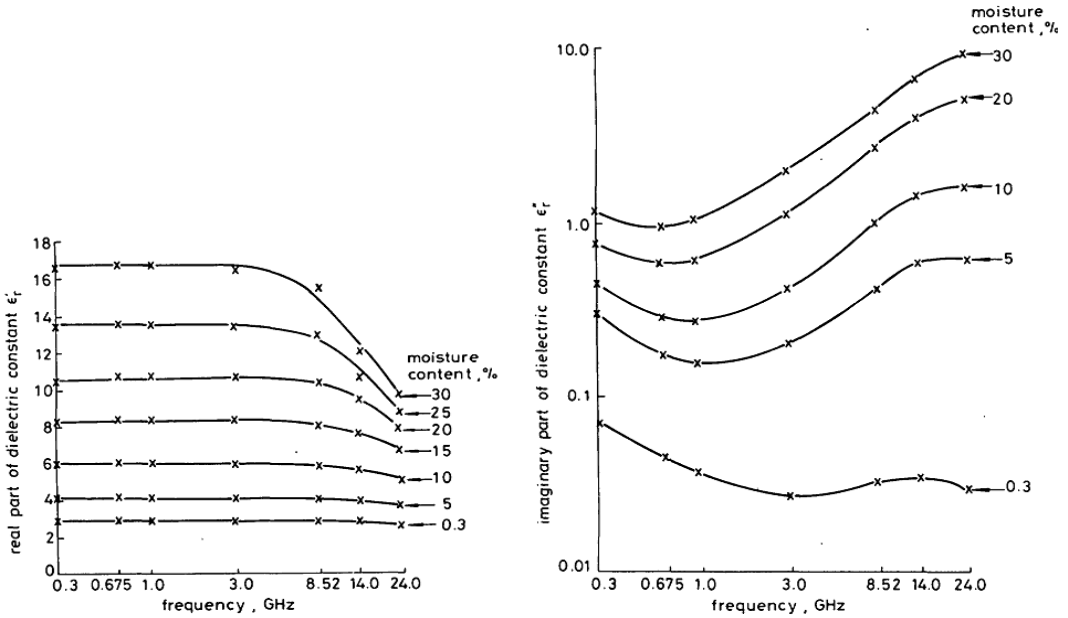

Figure 2.11: Measurement of real and imaginary parts of the complex dielectric constant of dust samples with different moisture contents as a function of frequency. [8]

Ansari and Evans [8] also reported that at 19.35 GHz, the silty clay loam sample's dielectric constant sharply increased for a 20% moisture content, as shown in Figure 2.12. The sharp increase of the real part can cause up to five times increment to the real part and up to 50 times to the imaginary value.

Sharif and Ghobrial [9] measured the dielectric constant of four different dust samples collected in the period between 1975 and 1982 at 8.3 GHz. The measurements are shown in Figure 2.13. In a similar observation to [8] it was deduced, both real and imaginary parts of the complex dielectric constant increase with

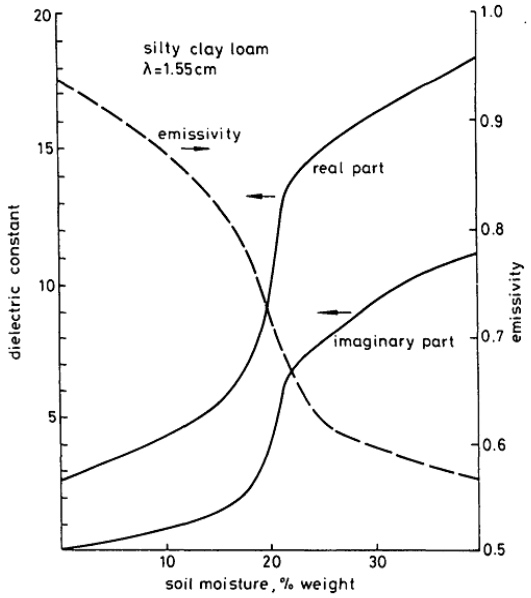

Figure 2.12: Variation of dielectric constant as a function of moisture content at 19.35 GHz. [8]

increasing the moisture content of the sample.

Furthermore,Sharif and Ghobrial [9] studied the frequency effects on the dielectric constant of two dust samples before and after dehydration. The conclusion derived from Figure 2.14 is that over a short frequency range, 8.2 - 9 GHz, both real and imaginary parts of the dust sample complex dielectric constant will not vary significantly. Ansari and Evans [8] reported that by changing frequency over a wide range, 0.3-24 GHz, the value of both real and imaginary parts of the dust complex dielectric constant can change significantly as shown in Figure 2.11.

As the dust samples' moisture content can significantly change the value of the dust dielectric constant, Sharif [4] gave the following equations for the dielectric constant of dust that is suspended in air with relative humidity of $\%H$:

$$\varepsilon'_H = \varepsilon' + 0.04H - 7.78 \times 10^{-4}H^2 + 5.56 \times 10^{-6}H^3 \tag{2.14a}$$

$$\varepsilon''_H = \varepsilon'' + 0.02H - 3.71 \times 10^{-4}H^2 + 2.76 \times 10^{-6}H^3 \tag{2.14b}$$

where $(\varepsilon' - j\varepsilon'')$ is the dry dust dielectric constant.

Dielectric Constant Assuming Ellipsoidal Dust particles

The dielectric constant of air with suspended ellipsoidal dust particles (dusty medium) requires more complex mathematical calculations as it requires the evaluation of the depolarisation factors along each of the ellipsoid axes. In this situation, the dust particles are much smaller than the propagating signal wavelength which permits the assumption of homogeneous and uniform medium [5].

The dusty medium electric constant, under the assumption of ellipsoidal dust particles, depends on the particles' intensity per unit volume of air and the propagating wave polarization relative to the particle axes.

To find the medium effective dielectric constant, Rai [10] defines the vector D as:

$$D = \varepsilon_0 E + P \tag{2.15}$$

where ε_0 is the permittivity of the free space, E is the incident electrical field and P is the polarisation per unit volume. Stratton [37] gave the relation between the incident electrical field and the vector D to be:

$$E = \frac{1}{\varepsilon_i} D \tag{2.16}$$

where ε_i is the effective dielectric constant of the medium having suspended dust particles.

Now we have [37]:

$$\varepsilon_i E = \varepsilon_0 E + Pv \tag{2.17}$$

where v is the relative volume fraction of the air occupied by dust particles.

From Equation 2.17, the medium effective dielectric constant can be given by:

$$\varepsilon_i = \varepsilon_0 + \frac{Pv}{E} \tag{2.18}$$

and the polarisation is given by [37] as:

$$P = \frac{E}{A_i + \frac{1}{\varepsilon - \varepsilon_0}};\ i = 1, 2, 3 \tag{2.19}$$

where ε is the dielectric constant of the dust particle and A_i is the depolarisation factor along a_i axis, Figure 2.1, and is given by [37] and [10]:

$$A_i = \frac{a_1 a_2 a_3}{2} \int_0^\infty \frac{\mathrm{d}s}{(s + a_i^2)\sqrt{(s + a_1^2)(s + a_2^2)(s + a_3^2)}};\ i = 1, 2, 3 \tag{2.20}$$

a_1, a_2, a_3 are the axes of the ellipsoidal dust particle as shown in Figure 2.1.

For the dusty medium, air with suspended dust particles, the effective dielectric constant can be given as [5] and [10]:

$$\varepsilon_i = 1 + \frac{v(\varepsilon - 1)}{1 + A_i(\varepsilon - 1)} \tag{2.21}$$

2.3 Conclusions

The dust particles have random and irregular shapes that do not have any particular symmetry. The shapes vary between needle-like to disc, sphere or ellipse shapes. The assumption that all dust particles have ellipsoidal shapes with different axes ratios gives three degrees of freedom and provide a good approximation to the realistic dust particles shapes. In addition, it will increase the mathematical complexity of the attenuation prediction models.

Under the assumption that all the dust particles have spherical shapes, the dust

particles' radii vary between 0.1 μm to 50 μm following different vertical size distributions as the radii decreases with the height. As shown in the chapter, the dust particles' size distribution differs from one geographical area to another and sometimes from one storm to another. According to Alhaider et al. [6] experimental results for Riyadh, Saudi Arabia, the dust particles' size distribution at measurement height of 21 metres is either normal or log-normal distributions. It can be concluded that the type of dust particles' vertical distribution depends mainly on the storm parameters, especially the wind speed, storm originating geographical area and soil conditions.

The difficulties involved in measuring dust mass concentration lead to the use of the optical visibility, which is easier to be measured, in order to evaluate the attenuation. The visibility is inversely proportional to the dust mass concentration. It increases with the height, Equation 2.12 is believed to show the right relation, as the dust particles become smaller and their mass concentration decreases. The two constants governing the relation between visibility and the mass concentration, C and γ, will have different values for different geographical area and mainly depend on erosion location, wind speed and soil conditions.

The measurements of the dust dielectric constant in the literature were made for collected dust samples. When evaluating the attenuation to the propagating microwave signal in a dusty medium, the dielectric constant of the air-dust mixture must be used. The mixture's dielectric constant can be found by using any of the mixing rules. Using the measured dust dielectric constant without considering the mixture may lead to errors in the attenuation prediction as the dielectric constant is an important factor in the attenuation calculation.

The dust moisture content, and hence the dust storm, has a large effect on the dielectric constant values. This can be seen from the reported dust samples, with different moisture content, dielectric constants measurements. So, the value of the dust dielectric constant can vary significantly with the dust moisture content and also with the incident wave frequency.

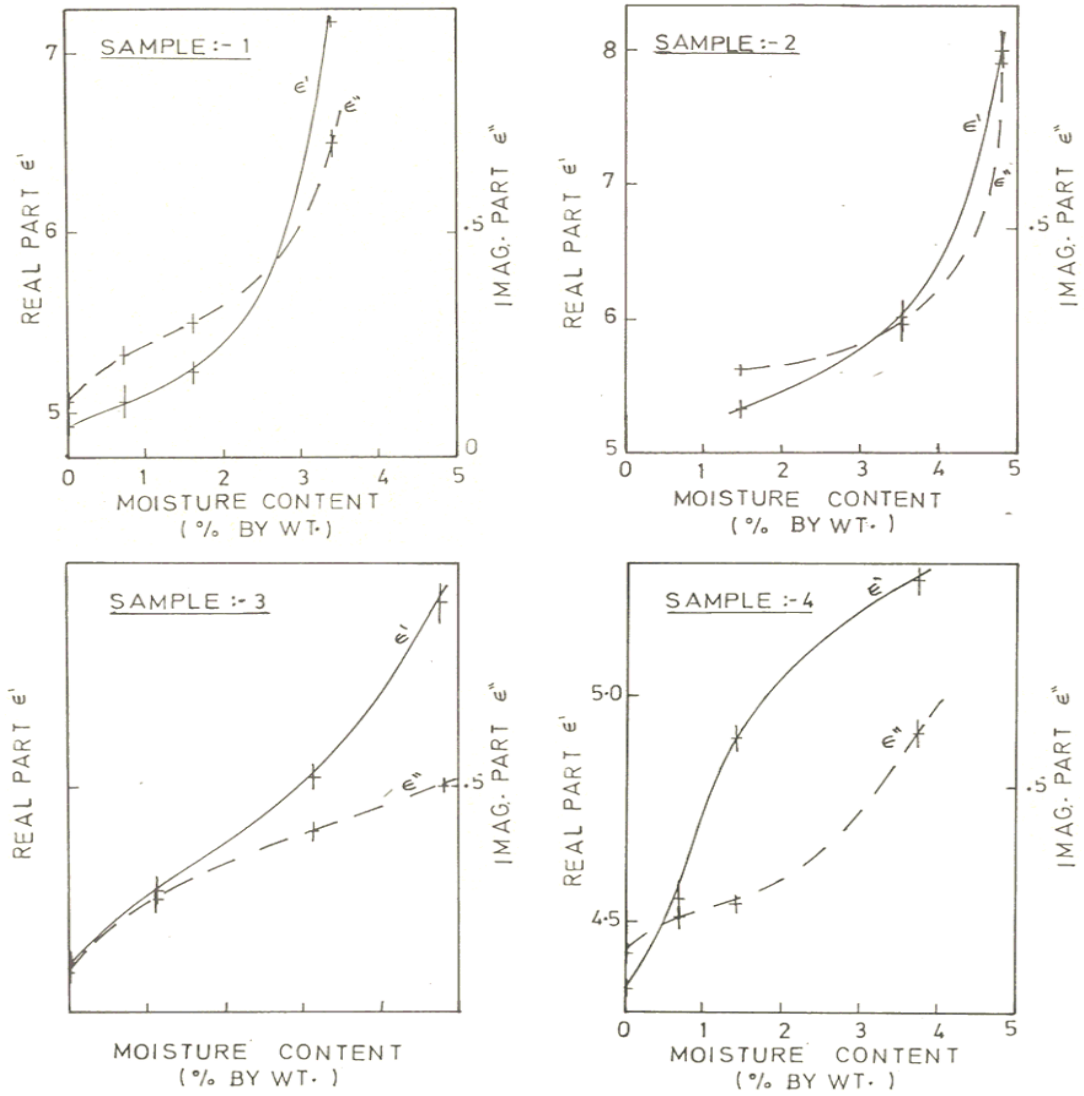

Figure 2.13: Measurement of real and imaginary parts of the complex dielectric constant of dust samples with different moisture contents at 8.3 GHz. [9]

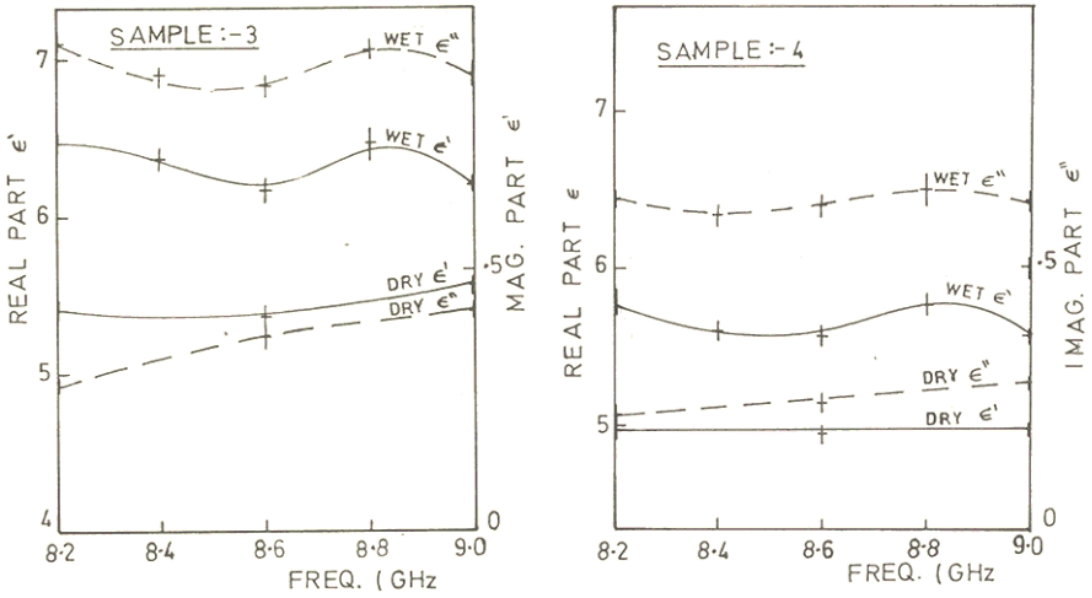

Figure 2.14: Effect of frequency change on the real and imaginary parts of the complex dielectric constant for two dust samples before and after dehydration. [9]

Chapter 3

Attenuation and Phase Shift Prediction Models

The first section of this chapter serves as a brief review of the scattering theorem. Due to the fact that the dust particles are tiny, the ratio of the particles radii to the incident signal wavelength is much smaller than 1, i.e. the validity of Rayleigh approximation is confirmed. As a result, the scattering due to these particles falls in the Rayleigh scattering regime. Eight attenuation and phase shift prediction models, of which six are based on the validity of Rayleigh approximation, are reviewed in this chapter.

The Rayleigh assumption encounters some limitation as the incident signal frequency increases which affect the models prediction performance. As the incident wave frequency increases, the Rayleigh-based models tend to underestimate the attenuation compared to the few measurements available in the literature.

Due to the limitations that are involved with Rayleigh approximation, few authors, Abdulla et al. [23], derived an attenuation model that uses the well-known Mie scattering solution, i.e. they assume the scattering of a microwave signal due to dust particle fall under the Mie scattering type. This assumption is theoretically invalid as the particle radii to the propagating wave wavelength ratio is very small compared to 1.

Both Rayleigh-based and Mie solution-based prediction models are developed under the assumption that all dust particles have spherical shapes. In nature, the dust particles shapes are random and may vary from needle-like to sphere, disc or sphere. Due to this fact, some of the authors, Ghbrial and Sharif [5], Dong et al. [25] and Rai [10], developed attenuation models under the assumption of ellipsoidal dust particles. This assumption provides three degrees of freedom and covers a wide range of shapes as the axes' ratios change. The only disadvantage of this assumption is that it increases the mathematical complexity of the model. Three derived attenuation and phase shift prediction models are presented in this chapter.

3.1 Scattering Theory

Scattering of propagating EM wave occurs when the wave is forced to deviate from straight line propagation by one or more localised non-uniformities in the propagation path. Scattering of EM wave is often accompanied by absorption [19]. Both scattering and absorption remove energy, attenuate, from the EM wave propagating through a medium. The attenuation of the propagating EM wave is also called extinction. According to Hulst [19], the extinction can be defined as:

$$\text{Extinction} = \text{Scattering} + \text{Absorption} \tag{3.1}$$

Scattering of the EM wave can be split into three main domains based on a dimensionless size parameter α, $\alpha = \frac{2\pi r}{\lambda}$; where r is the particle radius and λ is the wave length of the propagating EM wave. The three domains are:

$$\alpha = \begin{cases} \frac{2\pi r}{\lambda} \ll 1 & \text{Rayleigh Scattering (small particle compared to wavelength of light)} \\ \frac{2\pi r}{\lambda} \approx 1 & \text{Mie Scattering (particle about the same size as wavelength of light)} \\ \frac{2\pi r}{\lambda} \gg 1 & \text{Geometric Scattering (particle much larger than wavelength of light)} \end{cases}$$

Due to the fact that the dust particles have small radii that range between 0.1μ [4] and 50μ, the scattering of the propagating EM wave, with frequency up to $\approx$ 500 GHz, will fall in the Rayleigh scattering domain. This conclusion has some limitations that will be discussed later in this chapter.

In theory, the only scattering domain that is applicable to the dust particles is the Rayleigh scattering. One of the models discussed in this chapter considers the Mie scattering domain. The following paragraph illustrates the difference in scattering behaviour between Rayleigh scattering domain particles and the Mie scattering domain particles.

As the incident propagating wave interacts with the dust particle, the dust particle absorbs some energy. As a result, the particle becomes as a point source and starts re-radiating the energy in all directions. The scattered wave spatial distribution depends on the particle size parameter.

3.2 Attenuation Prediction Models

During the last 50 years, several efforts have been made to develop mathematical models to predict the attenuation of an EM wave propagating in a dusty medium. These models are either:

- Based on Rayleigh scattering approximation.

- Based on Mie scattering theory (Mie extinction formula) .

- Utilize the effective material property technique and general formulation of the complex propagation factor.

3.2.1 Rayleigh Scattering Based Models

Attenuation assuming spherical dust particles

CHU, August, 1978 [15]

Chu [15] considered the dust particles to have radii up to 50 μm. Due to their tiny sizes, and hence light weights, they can be blown by wind to heights of more than 1 km, it can reach up to 5 km [16]. On the other hand, larger particles, sand particles, are driven by wind as low-flying objects, typically up to 2-5 metres high. As a result, only the dust particles will have effects on the radio communication as the radio communication antennas are more than 5 m high. Chu [15] investigated the effects of dust on the radio communications.

The uncertainty involved in both the value of dust dielectric constant and the dust particles size distributions limits the accuracy of the models that aim to predict the attenuation and the phase shift that will occur to a wave propagating in a dusty medium. However, Chu [15] investigated the dust storm effects, attenuation and phase shift, dependence on the wave frequency.

The dust density in a dust storm forms an important factor when predicting the attenuation due to a dust storm. Since the density is very difficult to measure, the optical visibility forms a convenient measure to predict the dust density.

The visibility is inversely proportional to the optical attenuation- extinction- (dust storm attenuation at optical wavelength) coefficient and is given by Alhaider et al. [6] as:

$$\alpha_0 = 4.343 \frac{\ln |\frac{1}{k}|}{V} \tag{3.2}$$

α_0 = dust storm attenuation at optical wave length.

k = is the threshold contrast which is defined as: contrast ratio between black object and a bright background, Alhaider et al. [6] or the normalized difference in luminance between the sky and a mark located at the visibility distance, Chu [15] and Goldhirsh [21]. There is no world-wide standard value of k. However, Alhaider et al. [6] reported the value (0.02) and Chu [15], Goldhirsh [21] and Alhaider et al. [6] reported the value of (0.031) as the experiment-measured median.

Using the value $k = 0.031$ will give 15 dB as a proportionality constant between optical attenuation and visibility.

In addition, Chu [15] assumes that all the dust particles are in spherical shapes with different radii from storm to storm. This assumption is not true since the dust particles have random shapes that are far from spherical most of the time. In addition, Chu [15] performed his analysis on assuming dust particles to have radii that range between 10 μm and 100 μm. While Haddad et al. [3] reported that 30 % of the flying dust particles in dust storms have radii less than 5 μm.

Further, Chu [15] assumed all dust particles in a dust storm have a single radius (equisized particles). This assumption is not valid since the dust particles radii follow certain vertical distribution functions as discussed in Chapter II.

Chu [15] also assumed that dielectric constants take only one of two values; this is inconsistent with different authors' dielectric constant measurements shown in Chapter II. It is clear that the dielectric constant has a wide range of values that depend on many factors as discussed in Chapter II and cannot be assumed to have only one or two values.

Since the constant $(2\pi r)$, where r is the particle radius, is much less than the wavelength of centimetre and millimetre waves, the Rayleigh approximation is still valid.

A sand/dust storm attenuation is the sum of extinction cross-sections $C(r)$ of the spherical particles and is given by [15]:

$$A = \int_0^\infty N(r)C(r)\mathrm{d}r \tag{3.3}$$

where $N(r)dr$ is the number density within the radii range of r to $r + dr$.

Following Chu [15] derivation, the number of sand/dust particles per unit volume can be given by:

$$N = \frac{\alpha_0 r}{6.5\left(\frac{4}{3}\pi r^3\right)} \qquad \left[\#\text{particles/m}^3\right] \tag{3.4}$$

where α_0 in this equation is in dB/m.

The complex dust particle dielectric constant is given by:

$$\varepsilon = \varepsilon' - j\varepsilon'' \tag{3.5}$$

Following Chu [15] mathematical derivations, he arrived at the following formulas for the attenuation and phase shift coefficients:

$$A = \frac{3k}{13}\ \alpha_0\ r\ \ Im\left[\frac{\varepsilon - 1}{\varepsilon + 2}\right](8.686) \qquad \text{[dB/km]} \tag{3.6a}$$

$$= \frac{12.5944}{\lambda}\ \alpha_0\ r\ \ \left[\frac{3\varepsilon''}{\left(\varepsilon' + 2\right)^2 + \varepsilon''^2}\right] \qquad \text{[dB/km]} \tag{3.6b}$$

$$\Phi = \frac{3k}{13}\ \alpha_0\ r\ \ Re\left[\frac{\varepsilon - 1}{\varepsilon + 2}\right]\left(\frac{180}{\pi}\right) \qquad \text{[deg/m]} \tag{3.6c}$$

$$= \frac{83.077}{\lambda}\ \alpha_0\ r\ \ \left[\frac{\varepsilon'^2 + \varepsilon''^2 + \varepsilon' - 2}{\left(\varepsilon' + 2\right)^2 + \varepsilon''^2}\right] \qquad \text{[deg/km]} \tag{3.6d}$$

where $k = \frac{2\pi}{\lambda}$, V is the visibility in kilometres, λ is the incident wave wavelength in metres and r is the effective radius of the dust particles in metres. In the source paper, Chu [15], the specified units for the attenuation and phase shift are [dB/m] and [deg/km] respectively. After interpolating from attenuation and

phase shift figures in [15], it was found out that the units are [dB/km] and [deg/km] as indicated in Equation 3.5.

By using Equation 3.2, the attenuation and the phase shift can be written as:

$$A = \frac{566.748}{V\lambda} \; r \; \left[\frac{\varepsilon''}{(\varepsilon'+2)^2 + \varepsilon''^2}\right] \qquad \text{[dB/km]} \tag{3.7a}$$

$$\Phi = \frac{1246.155}{V\lambda} \; r \; \left[\frac{\varepsilon'^2 + \varepsilon''^2 + \varepsilon' - 2}{(\varepsilon'+2)^2 + \varepsilon''^2}\right] \qquad \text{[deg/km]} \tag{3.7b}$$

Ansari and Evans, October, 1982 [8]

Ansari and Evans [8] mentioned that 30% of the population (particles) of the dust in a dust storm will have radii of less than 5 μm as per study performed in Sudan. They assumed that dust particles will have radii of $\leq$ 100 μm. But, from the literature review in Chapter II, the particles of radii more than 50 μ is counted as large particles, sand particles, and is difficult to be elevated by wind to more than few metres. So, their effect on radio propagation can be ignored.

Ansari and Evans [8] derived the formulas of the attenuation and the phase shift due to dust storms by following similar method to the one used to derive similar equations for rain and ice in the troposphere. Following this method may lead to some degree of inaccuracy as the dust particles are tiny compared to rain and ice particles. This method leads to a rise of the forward propagation constant for both horizontally and vertically polarised propagating wave. This forward propagation constant can be given by Ansari and Evans [8] as:

$$K_{V,H}(\theta) = k + \lambda \int_0^\infty f_{V,H}(\theta, r) p(r) dr \tag{3.8}$$

where V and H indicate vertically and horizontally polarised incident waves respectively, $k = \frac{2\pi}{\lambda}$, θ is the incident wave elevation angle, $f_{V,H}(\theta, r)$ is the scattering amplitude and $p(r)dr$ is the particle size distribution per unit volume, in (cm^3), of particles that have radii in the range $r \rightarrow r + dr$.

The attenuation and the phase shift can be found as [8]:

$$A_{V,H} = 8.686 \times 10^5 Im[K_{V,H}(\theta)] \qquad \text{[dB/km]} \tag{3.9a}$$

$$\Phi_{V,H} = \frac{180}{\pi} \times 10^5 Re[K_{V,H}(\theta)] \qquad \text{[deg/km]} \tag{3.9b}$$

Ansari and Evans [8] compared the calculated scattering amplitudes of particles with radii = 100 μm for two different geometrical shapes, spheres and spheroids, under the assumption of validity of Rayleigh approximation at 37 GHz to the exact calculations using Fredholm Integral Method (FIM), derived by Ansari and Evans for rain and ice attenuation calculation, as shown in Table 3.1. This comparison revealed, due to tiny difference, that the Rayleigh approximation is valid for dust particles up to a frequency of 37 GHz [8].

Table 3.1: Comparison of scattering amplitudes between Rayleigh based and exact methods for sand/dust particles with radii of 100 μm and at frequency of 37 GHz for both sphere and speriod particles. [8]

	Spheres		Spheroids	
Dielectric constant (Loamy fine sand)	Rayleigh	FIM	Rayleigh	FIM
$2.53 - j0.0625$ (0% moisture content)	2.033×10^{-5} $+j5.4968 \times 10^{-7}$	2.03561×10^{-5} $+j5.54645 \times 10^{-7}$	$f_H = 1.6232 \times 10^{-5}$ $+j3.8414 \times 10^{-7}$ $f_V = 2.5915 \times 10^{-5}$ $+j9.7997 \times 10^{-7}$	$f_H = 1.6243 \times 10^{-5}$ $+j3.8598 \times 10^{-7}$ $f_V = 2.59517 \times 10^{-5}$ $+j9.86853 \times 10^{-7}$
$4.0 - j1.325$ (10% moisture content)	3.1485×10^{-5} $+j6.335 \times 10^{-6}$	3.15546×10^{-5} $+j6.3794 \times 10^{-6}$	$f_H = 2.3668 \times 10^{-5}$ $+j3.8734 \times 10^{-6}$ $f_V = 4.8509 \times 10^{-5}$ $+j1.8038 \times 10^{-5}$	$f_H = 2.3681 \times 10^{-5}$ $+j3.8869 \times 10^{-6}$ $f_V = 4.86307 \times 10^{-5}$ $+j1.81768 \times 10^{-5}$
$7.375 - j4.15625$ (20% moisture content)	4.4079×10^{-5} $+j7.1342 \times 10^{-6}$	4.42473×10^{-5} $+j7.23512 \times 10^{-6}$	$f_H = 3.0863 \times 10^{-5}$ $+j3.7933 \times 10^{-6}$ $f_V = 9.4221 \times 10^{-5}$ $+j4.1626 \times 10^{-5}$	$f_H = 3.0902 \times 10^{-5}$ $+j3.8217 \times 10^{-6}$ $f_V = 9.46887 \times 10^{-5}$ $+j4.22671 \times 10^{-5}$

The authors consider two cases when deriving the propagation constant equation. First, they assumed that all particles in the medium have the same size. The second case considered the availability of particles size distribution. In the first case, using Rayleigh approximation, since the particles size parameter $\ll 1$, and using Equation 3.4, the propagation constant can be expressed as [8]:

$$K = k\left[1 + \frac{3.46r}{V}\left(\frac{\varepsilon - 1}{\varepsilon + 2}\right)\right] \tag{3.10}$$

where r is particles' effective radius and V is the visibility. Look to the source paper by Ansari and Evans [8] for detailed derivation. The attenuation and the phase shift given by the authors, Equation 3.8, show multiplications to 10^5 for both attenuation and phase shift. By working through the paper again and using λ, r in metres and the visibility in kilometres, the multiplication will be cancelled. The attenuation and the phase shift under the assumption of equisized spherical dust scatterers can be then written as:

$$A = \frac{566.497}{V\lambda}\ r\ \left[\frac{\varepsilon''}{(\varepsilon' + 2)^2 + \varepsilon''^2}\right] \quad \text{[dB/km]} \tag{3.11a}$$

$$\Phi = \frac{360}{\lambda} + \frac{1.2456 \times 10^3}{V\lambda}\ r\ \left[\frac{\varepsilon'^2 + \varepsilon''^2 + \varepsilon' - 2}{(\varepsilon' + 2)^2 + \varepsilon''^2}\right] \quad \text{[deg/km]} \tag{3.11b}$$

As it is clear from the phase shift formula, ignoring the fist right-hand term will not have any effect on the final phase shift value.

By considering that the particles size distribution to follow an exponential distribution, as per analysis done in Sudan and reported by Ansari and Evans [8], of the type:

$$P(r) = \beta \exp(-\beta r) \tag{3.12}$$

with a mean value $\overline{a} = 1/\beta$.

Using the fact that the optical extinction = 2, the propagation coefficient can be expressed as [8]:

$$K = k\left[1 + \frac{45}{8.686\beta V}\left(\frac{\varepsilon - 1}{\varepsilon + 2}\right)\right] \tag{3.13}$$

Following the same mathematical derivation of Equation 3.10, for equisized spherical scatterers, the attenuation and the phase shift can be written as:

$$A = \frac{848.23}{\beta V \lambda}\ r\ \left[\frac{\varepsilon''}{(\varepsilon' + 2)^2 + \varepsilon''^2}\right] \qquad \text{[dB/km]} \tag{3.14a}$$

$$\Phi = \frac{360}{\lambda} + \frac{1.8651 \times 10^3}{\beta V \lambda}\ r\ \left[\frac{\varepsilon'^2 + \varepsilon''^2 + \varepsilon' - 2}{(\varepsilon' + 2)^2 + \varepsilon''^2}\right] \qquad \text{[deg/km]} \tag{3.14b}$$

Again it is clear from the phase shift formula, ignoring the fist right-hand term will not have any effect on the final phase shift value.

J. Goldhirsh, November, 1982 and December 2001 [21] [22]

If the dusty medium is assumed to be a monodispersive system, where all dust particles are spheres with equal radii, the attenuation that will occur to a propagating microwave signal in this medium is expressed by Chu [15] as in Equation 3.6. Using Equation 3.4, the attenuation can be given by [21]:

N.B.: In [21], the constant in equation 16 should be $3,67 \times 10^{-2}$.

$$A(\lambda) = \frac{1.0287 \times 10^6}{\lambda} N r^3\ \left[\frac{\varepsilon''}{(\varepsilon' + 2)^2 + \varepsilon''^2}\right] \qquad \text{[dB/km]} \tag{3.15}$$

If the particle size distribution (more realistic polydispersive system) is taken into consideration, the attenuation expression can be written as [21]:

$$A(\lambda) = \frac{1.0287 \times 10^6}{\lambda}\ \left[\frac{\varepsilon''}{(\varepsilon' + 2)^2 + \varepsilon''^2}\right] \sum_i N_i r_i^3 \qquad \text{[dB/km]} \tag{3.16}$$

where N_i is the number of particles with radii ranging between r_i and $r_i + dr_i$ per cubic metre. If the Equation 3.16 is multiplied and divided by the total particles density N, the attenuation can be written as [21]:

$$A(\lambda) = \frac{1.0287 \times 10^6}{\lambda} \; N \; \left[\frac{\varepsilon''}{(\varepsilon' + 2)^2 + \varepsilon''^2}\right] \sum_i P_i r_i^3 \qquad \text{[dB/km]} \tag{3.17}$$

where $P_i = N_i/N$: is the probability that r_i falls between r_i and $r_i + dr_i$.

Using Equations 3.2 and 3.4, the relation between the visibility and the total particles density can be written as [21]:

$$V = \frac{5.509 \times 10^{-4}}{N r^2} \qquad \text{[km]} \tag{3.18}$$

and the attenuation can be expressed as:

$$A(\lambda) = \frac{566.7108}{V\lambda} \; \left[\frac{\varepsilon''}{(\varepsilon' + 2)^2 + \varepsilon''^2}\right] \qquad \text{[dB/km]} \tag{3.19}$$

Later Goldhirsh in 2001 [22] predicts that his attenuation models (above) that are based on Rayleigh approximation are valid since Rayleigh approximation holds for frequencies up to ≈ 48 GHz.

The total relative volume of dust particles in air were given by J. Goldhirsh, 2001, [22] as:

$$v = \frac{4}{3}\pi \sum_i N_i r_i^3 \qquad \left[\text{m}^3 \text{ of dust/ } \text{m}^3 \text{ of air}\right] \tag{3.20}$$

Then, from Equation 3.16, the attenuation can be expressed as:

$$A(\lambda) = \frac{2.456 \times 10^5}{\lambda} \; \left[\frac{\varepsilon''}{(\varepsilon' + 2)^2 + \varepsilon''^2}\right] .v \qquad \text{[dB/km]} \tag{3.21}$$

which is similar expression to the one derived by Ghobrial and Sharif [5].

As the dust mass concentration (M), relative dust mass per cubic volume of air, is given by [22]:

$$M = \rho.v \qquad \left[\text{kg of dust/m}^3 \text{ of air}\right] \tag{3.22}$$

where ρ is the dust density in kg/m^3 and v is the total volume fraction of the air that is filled with dust.

Using the relation between mass concentration and visibility given by Patterson and Gillette [13]:

$$M = \frac{C}{V^{\gamma}} \longrightarrow v = \frac{C}{\rho V^{\gamma}} \tag{3.23}$$

where C and γ are constants explained in Chapter II. From Equation 3.21, the attenuation can be given as:

$$A(\lambda) = \frac{2.456 \times 10^5}{\lambda} \left[\frac{\varepsilon''}{(\varepsilon'+2)^2 + \varepsilon''^2}\right].\frac{C}{\rho V^{\gamma}} \qquad \text{[dB/km]} \tag{3.24}$$

and similarly, the phase shift can be given by:

$$\Phi = \frac{5.4 \times 10^5}{\lambda} \left[\frac{\varepsilon'^2 + \varepsilon''^2 + \varepsilon' - 2}{(\varepsilon'+2)^2 + \varepsilon''^2}\right].\frac{C}{\rho V^{\gamma}} \qquad \text{[deg/km]} \tag{3.25}$$

Goldhirsh [22] used the values $\rho = 2.44 \times 10^3$ [kg/m^3], $C = 2.3 \times 10^{-5}$ [kg.km/m^3] and $\gamma = 1.7$ which are believed to be right values for Sudan as reported by Ghobrial and Sharif [5]. These values are taken directly from the paper by Patterson and Gillette [13] and believed to be right for Sudan as the dust is not generated locally and tropical climatic conditions dominate, as reported by Sharif [4].

Due to huge differences between geographical locations of dust storms, these values are not applicable always and may differ from one geographical area to another. In the above derivations, the equation of the relative dust volume is

replaced by the original symbols, not values, to work for different geographical locations. Deep study of the dust storm properties, dust storm originating region and the geographical location where the dust storm spreads are required to achieve the right values of these constants.

Haddad et al., June, 1983 [3]

Haddad et al. [3] followed exactly the same procedure followed by Chu [15] and arrive to an identical result represented by Equation 3.10.

Ghobrial and Sharif, October, 1985 [5]

Ghobrial and Sharif [5] found that the following values are believed to be applicable for Sudan:

$\rho = 2.44 \times 10^3$ [kg/m^3], $C = 2.3 \times 10^{-5}$ [g.km/m^3], $\gamma = 1.07$

They used these values and derived an equation, Equation 3.23, that relates the relative volume occupied by the dust particles in a storm to the visibility, based on the relation between the dust mass concentration and visibility, given in Chapter II, derived by Patterson and Gillette [13]. They found the attenuation, under the assumption of spherical dust particles, can be give by equation 3.21 [5].

Later, in 2001, J. Goldhirsh [22] used the derived relation between the relative occupied volume by the dust particles and the visibility and then he derived an equation for the attenuation, Equation 3.24.

Alhaider et al., September, 1987 [6]

Alhaider et al. [6] consider the dust particles to be the particles with radii $\leqq 50$ μm, and hence the Rayleigh approximation holds for the dust particles. Alhaider et al. [6] showed that the attenuation of a millimetre wave propagating in a dusty medium can be given by Equation 3.17. This equation requires the knowledge of the number of dust particles in a dust storm or the relative volume fraction of the storm that is filled with dust which is difficult to be measured. By rearranging Equation 3.4, Alhaider et al. [6] used the following form for the optical attenuation:

$$\alpha_0 = 4.343 \times 10^3 \, (2\pi N) \sum_i P_i r_i^2 \qquad \text{[dB/km]} \tag{3.26}$$

After that, Alhaider et al. [6] used Equation 3.26 together with the Equation 3.2 and arrived at the following equation for the attenuation:

$$A = 566.97 \left(\frac{1}{V}\right) \left(\frac{r_e}{\lambda}\right) \left[\frac{\varepsilon''}{(\varepsilon' + 2)^2 + \varepsilon''^2}\right] \qquad \text{[dB/km]} \tag{3.27}$$

where r_e is the effective particles' radii and is given by [6]:

$$r_e = \frac{\sum_i P_i r_i^3}{\sum_i P_i r_i^2} \tag{3.28}$$

Y. Yan, August, 2004 [38]

Yan [38] gave the equations of the real and imaginary parts of the effective dielectric constant of a dust storm, Equation 3.5, to be:

$$\varepsilon' = \frac{1 + 3v \, (\varepsilon'_d - 1) \, (\varepsilon'_d + 2) + \varepsilon''_d}{(\varepsilon''_d + 2)^2 + \varepsilon''^2_d} \tag{3.29a}$$

$$\varepsilon'' = \frac{9v\varepsilon''_d}{(\varepsilon''_d + 2) + \varepsilon''^2_d} \tag{3.29b}$$

where ε'_d and ε''_d are the real and imaginary parts of the measured dust dielectric constant and v is the relative volume fraction of a dust storm that is filled by dust. The author did not give any equation for the relative volume of the dust. In this report, it is assumed that the relative volume can be found using Equation 3.23. The author assumes that the dusty medium can be accepted as even media, based on the equivalent media propagation theory. The propagation constant of the dust storm is given by [38]:

$$\Gamma = \alpha + j\beta \tag{3.30}$$

where α is the attenuation (A) and β is the phase shift (Φ). Assuming that all dust particles have the same size, Yan [38] gave the following equations for the attenuation and the phase shift:

$$A = 3.431 \times 10^6 f N r^3 \left[\frac{\varepsilon''}{(\varepsilon'+2)^2+\varepsilon''^2}\right] \quad \text{[dB/km]} \tag{3.31a}$$

$$\Phi = 7.545 \times 10^6 f N r^3 \left[\frac{(\varepsilon'-1)(\varepsilon'+2)+\varepsilon''^2}{(\varepsilon'+2)^2+\varepsilon''^2}\right] \quad \text{[deg/km]} \tag{3.31b}$$

where f is the frequency, in GHz, of the of the propagating wave (incident wave). The attenuation formula above is identical to Equation 3.15. The phase shift is similar to the one derived by Chu [15]. This phase shift can be achieved by substituting Equations 3.2 and 3.4 into Equation 3.6. By considering a more realistic case where the dust particles have different sizes following some particles size distribution (polydispersive system) and using Equation 3.16, the attenuation can be given by:

$$A = 3.431 \times 10^6 f \left[\frac{\varepsilon''}{(\varepsilon'+2)^2+\varepsilon''^2}\right] \sum_i N_i r_i^3 \quad \text{[dB/km]} \tag{3.32}$$

$$A = 8.191 \times 10^5 \ f \ \left[\frac{\varepsilon''}{(\varepsilon'+2)^2+\varepsilon''^2}\right] .v \quad \text{[dB/km]} \tag{3.33}$$

Then, by using Equation 3.21, the attenuation can be rewritten as:

$$A = 8.191 \times 10^5 f \left[\frac{\varepsilon''}{(\varepsilon'+2)^2+\varepsilon''^2}\right] \left(\frac{C}{\rho V^\gamma}\right) \quad \text{[dB/km]} \tag{3.34}$$

Following the same procedures, the phase shift can be given by:

$$\Phi = 1.80 \times 10^6 \ f \ \left[\frac{(\varepsilon'-1)(\varepsilon'+2)+\varepsilon''^2}{(\varepsilon'+2)^2+\varepsilon''^2}\right] \left(\frac{C}{\rho V^\gamma}\right) \quad \text{[deg/km]} \tag{3.35}$$

Dong et al., May, 2012 [25]

Dong et al. [25] used similar assumptions and similar method used by Ansari and Evans [8]. Using Equation 3.21, Dong et al. [25] arrived to the following equation for the propagation coefficient:

$$K = k + \frac{3\pi}{\lambda}\left(\frac{\varepsilon - 1}{\varepsilon + 2}\right).v \tag{3.36}$$

Using Equations 3.11, 3.12, 3.23 and 3.36, Dong et al. [25] arrived at the following equation for the attenuation:

$$A = 8686Im\left[K\right] = 8.1864 \times 10^5 \;\; F \;\; \left[\frac{\varepsilon''}{(\varepsilon' + 2)^2 + \varepsilon''^2}\right] \;\; \left(\frac{C}{\rho V^\gamma}\right) \qquad \text{[dB/km]} \tag{3.37}$$

where the incident wave frequency F is in GHz. Similarly, the phase shift can be given by:

$$\Phi = \frac{1.8 \times 10^5}{\pi} Re\left[K\right] = \frac{360}{\lambda} + 1.8 \times 10^6 \;\; F \;\; \left[\frac{\varepsilon'^2 + \varepsilon''^2 + \varepsilon' - 2}{(\varepsilon' + 2)^2 + \varepsilon''^2}\right] \;\; \left(\frac{C}{\rho V^\gamma}\right) \qquad \text{[deg/km]} \tag{3.38}$$

The first right-hand term of the phase sift equation can be ignored.

Dong et al. [25] used the values of constants C and γ that are applicable for Sudan in his derivation. These values are not applicable for all different geographical areas. In this report, all values are replaced by their symbols which can then be replaced by the constants' right values.

Attenuation assuming ellipsoidal dust particles

Ghobrial and Sharif, October, 1985 [5]

The effective dielectric constant of a dusty medium, under the assumption of

ellipsoidal suspended dust particles, can be given by [5]:

$$\varepsilon_i = 1 + \frac{v(\varepsilon - 1)}{1 + A_i(\varepsilon - 1)};\ i = 1, 2, 3 \tag{3.39}$$

where A_i is the depolarization factor along the axis a_i of the ellipsoidal particle and can be given as, Stratton [37]:

$$A_i = \frac{a_1 a_2 a_3}{2} \int_0^\infty \frac{\mathrm{d}s}{(s + a_i^2)\sqrt{(s + a_1^2)(s + a_2^2)(s + a_3^2)}};\ i = 1, 2, 3 \tag{3.40}$$

The total relative volume of the dusty medium, that is occupied by the dust particles, in Sudan is very small even for dense dust storms, as demonstrated in Section 2.1.1. Hence, the second right-hand term of Equation 3.39 is much smaller than unity.

The propagation constant can be given by [5]:

$$\Gamma = \alpha_i + j\beta_i = j\frac{\omega}{c}\sqrt{\varepsilon_i} = j\frac{2\pi}{\lambda}\sqrt{\varepsilon_i} = j\frac{2\pi}{\lambda}\sqrt{\left[1 + \frac{v(\varepsilon - 1)}{1 + A_i(\varepsilon - 1)}\right]} \qquad i = 1, 2, 3 \tag{3.41}$$

and hence the attenuation and the phase shift constants along each axis of the ellipsoidal particle can be expressed as [5]:

$$\alpha_i = -\frac{\pi}{\lambda} Im\left[\frac{v(\varepsilon - 1)}{1 + A_i(\varepsilon - 1)}\right] \quad [\mathrm{dB/km}];\ i = 1, 2, 3 \tag{3.42a}$$

$$\beta_i = \frac{2\pi}{\lambda}\left[1 + \frac{1}{2} Re\left(\frac{v(\varepsilon - 1)}{1 + A_i(\varepsilon - 1)}\right)\right];\ i = 1, 2, 3 \tag{3.42b}$$

The unit of the phase shift was not reported. The phase shift per unit length relative to a wave travelling in air can be expressed as [5]:

$$\Phi_i = \frac{\pi}{\lambda} Re\left[\frac{v(\varepsilon-1)}{1+A_i(\varepsilon-1)}\right];\ i=1,2,3 \tag{3.43}$$

Due to the fact the the ellipsoidal dust particles are randomly oriented relative to the wave polarization, it is essential to obtain the average value of all α_i and β_i which is given by [5]:

$$\alpha_i = -\frac{\pi}{3\lambda}\sum_i Im\left[\frac{v(\varepsilon-1)}{1+A_i(\varepsilon-1)}\right] \quad [\text{dB/km}];\ i=1,2,3 \tag{3.44a}$$

$$\beta_i = \frac{\pi}{3\lambda}\sum_i Re\left(\frac{v(\varepsilon-1)}{1+A_i(\varepsilon-1)}\right);\ i=1,2,3 \tag{3.44b}$$

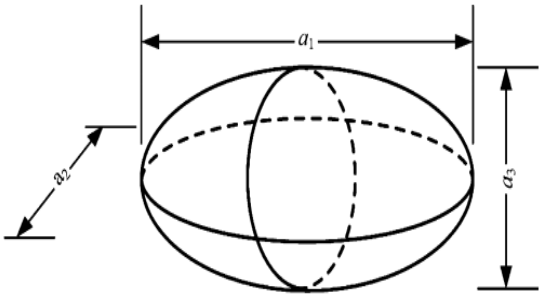

Figure 3.1: Dust particle ellipsoidal geometry approximation.

If the probability of finding particles with a_2/a_1 axes ratio, considering Figure 3.1 as an example of ellipsoidal dust particle, in the range $R_{p-1} < R < R_{p+1}$ is given as $P_p(R)$ and the probability of finding the particles with a_3/a_2 axes ratio in the range $r_{q-1} < r < r_{q+1}$ is given by $P_q(r)$. Then, the probability of finding particles with a_2/a_1 and a_3/a_2 axes ratios within given range will be $P_p(R)P_q(r)$.

-Attenuation and phase shift for a vertically polarised wave [5]

The electric field direction of a vertically polarized wave is parallel to the ellipsoidal dust particle's shortest axis, axis a_3 in Figure 3.1. The total attenuation and the phase shift constants, due to the presence of the ellipsoidal dust particles, for vertically polarised wave can be given by [5]:

$$\alpha_V = -\frac{\pi}{3\lambda}\sum_p\sum_q P_p P_q Im\left[\frac{v(\varepsilon-1)}{1+A_{i,p,q}(\varepsilon-1)}\right] \quad \text{[dB/km]} \tag{3.45a}$$

$$\beta_V = \frac{\pi}{3\lambda}\sum_p\sum_q Re\left[\frac{v(\varepsilon-1)}{1+A_{i,p,q}(\varepsilon-1)}\right] \tag{3.45b}$$

where i is the shortest axis in the dust particle, a_3 in Figure 3.1.

-Attenuation and phase shift for a horizontally polarised wave [5]

Since the ellipsoidal dust particles have no particular orientation in the horizontal plane, the attenuation and the phase shift is achieved by taking the average of the attenuation and phase shifts of the two horizontal axes as [5]:

$$\alpha_H = \frac{\alpha_x+\alpha_z}{2} = -\frac{\pi}{2\lambda}\sum_p\sum_q vP_pP_qIm\left[\frac{(\varepsilon-1)}{1+A_{x,p,q}(\varepsilon-1)}+\frac{(\varepsilon-1)}{1+A_{z,p,q}(\varepsilon-1)}\right] \quad \text{[dB/km]} \tag{3.46a}$$

$$\beta_H = \frac{\beta_x+\beta_z}{2} = \frac{\pi}{2\lambda}\sum_p\sum_q Re\left[\frac{(\varepsilon-1)}{1+A_{x,p,q}(\varepsilon-1)}+\frac{(\varepsilon-1)}{1+A_{z,p,q}(\varepsilon-1)}\right] \tag{3.46b}$$

where x and z are the other two axes of the ellipse - other than the shortest axis - axes a_1 and a_2 in Figure 3.1.

-Attenuation and cross polarization of a circularly polarised wave [5]

A circularly polarised wave can be resolved into two linearly polarised wave with equal magnitudes but with their polarization are 90° out of phase, orthogonal.

In a previous discussion it was shown that the attenuation for a vertically polarised wave propagating through a dusty medium is not the same as the one for a horizontally polarised wave propagating through the same medium. As a result, circular polarisation will be induced [5]. The cross-polarisation-discrimination

(XPD) for a circularly polarised wave is given by [5]:

$$XPD = 10\log_{10}\left|\frac{1+2m\cos\phi+m^2}{1-2m\cos\phi+m^2}\right| \tag{3.47}$$

where m is the two linearly polarised waves, that produce the circular polarization, magnitudes ratio and $\phi = 90°$ - phase difference between the two waves. If $m = 1$ and $\phi = 90°$, the wave is truly circularly polarised [5], XPD becomes infinite. For a wave propagating in a dusty medium, m and ϕ are given by [5]:

$$m = e^{|\alpha_H - \alpha_V|D} \tag{3.48a}$$

$$\phi = (\beta_H - \beta_V)D \tag{3.48b}$$

The attenuation of a circularly polarised wave propagating in a dusty medium is caused mainly due to two mechanisms: energy absorption in the medium and change in polarisation. The attenuation of a circularly polarised wave can be given as [5]:

$$\alpha_C = -20\log_{10}\sqrt{\frac{1+2m\cos\phi+m^2}{4}}\; e^{-\alpha_V D} \tag{3.49}$$

For a constant m, the maximum and the minimum attenuation caused by changes in the phase are given by [5]:

$$\alpha_{C_{max}} = -20\log_{10}\left[\frac{1-m}{2}\right]\; e^{-\alpha_V D} \tag{3.50a}$$

$$\alpha_{C_{max}} = -20\log_{10}\left[\frac{1+m}{2}\right]\; e^{-\alpha_V D} \tag{3.50b}$$

and these attenuations correspond to $\phi = \pi$ and 0 respectively.

Dong et al., May, 2012 [25]

The ellipsoidal dust particle forward-scattering amplitude, based on Rayleigh approximation, can be expressed as [25]:

$$f_i = k^2 \frac{a_1 a_2 a_3}{3} \left(L_i' - iL_i''\right) \tag{3.51}$$

where $k = \frac{2\pi}{\lambda}$, and:

$$L_i' = Re\left[\frac{1}{1 + A_i(\varepsilon - 1)}\right]; \quad L_i'' = Im\left[\frac{1}{1 + A_i(\varepsilon - 1)}\right]; \quad i = 1, 2, 3 \tag{3.52}$$

A_i is the depolarisation factor along each axis and is given by the Equation 3.40. The sum of all three depolarisation factors, $A_1 + A_2 + A_3 = 1$, is equal to one.

Using Equations 3.51 and 3.52, the propagation coefficient will be [25]:

$$K = k + \frac{\pi}{\lambda} L_i'.v - i\frac{\pi}{\lambda} L_i''.v \tag{3.53}$$

where v is the relative volume of the storm that is occupied by dust particles and given by Equation 3.35.

The attenuation and the phase shift coefficients, in terms of visibility, can be given by:

$$\alpha_i = 8686 Im\left[K\right] = 9.096 \times 10^4 \;\; F \;\; L_i'' \left[\frac{C}{\rho V^\gamma}\right] \qquad \text{[dB/km]}\,; \;\; i = 1, 2, 3 \tag{3.54a}$$

$$\beta_i = \frac{1.8 \times 10^5}{\pi} Re\left[K\right] = 6 \times 10^5 \;\; F \;\; L_i' \left[\frac{C}{\rho V^\gamma}\right] \qquad \text{[deg/km]}\,; \;\; i = 1, 2, 3 \tag{3.54b}$$

where F is the frequency in GHz and i indicates the ellipsoidal particle three axes, one (shortest axis) corresponds to vertical polarisation and the other two randomly oriented axes corresponds to horizontal polarisation. For example, if we assume axis number 3 is the shortest particle axis, then $i = 3$ corresponds

to the vertically polarised wave while $i = 1, 2$ correspond to the horizontally polarised wave.

-Attenuation and phase shift for a horizontally polarised wave [25]

As mentioned before, the two horizontal axes of the ellipsoidal dust particle are randomly oriented in the horizontal plane. As a result, the attenuation and phase-shift coefficients for the horizontally polarised wave, assuming axes 1 and 2 are the particle horizontal axes, can be expressed as:

$$\alpha_H = \frac{\alpha_1 + \alpha_2}{2} = 9.096 \times 10^4 \;\; F \;\; \left(\frac{L_1'' + L_2''}{2}\right) \left[\frac{C}{\rho V^\gamma}\right] \qquad \text{[dB/km]} \qquad (3.55a)$$

$$\beta_H = \frac{\beta_1 + \beta_2}{2} = 6 \times 10^5 \;\; F \;\; \left(\frac{L_1' + L_2'}{2}\right) \left[\frac{C}{\rho V^\gamma}\right] \qquad \text{[deg/km]} \qquad (3.55b)$$

-Attenuation and phase shift for a vertically polarised wave [25]

Assuming the particle's shortest axis is axis 3, the attenuation and the phase shift coefficients of the vertically polarised wave can be given by:

$$\alpha_V = 9.096 \times 10^4 \;\; F \;\; L_3'' \left[\frac{C}{\rho V^\gamma}\right] \qquad \text{[dB/km]} \qquad (3.56a)$$

$$\beta_V = 6 \times 10^5 \;\; F \;\; L_3' \left[\frac{C}{\rho V^\gamma}\right] \qquad \text{[deg/km]} \qquad (3.56b)$$

-Differential attenuation and phase shift [25]

The differential attenuation and phase shift can be written as:

$$\Delta\alpha = |\alpha_H - \alpha_V| = 9.096 \times 10^4 \;\; F \;\; \left|\frac{(L_1'' + L_2'') - L_3''}{2}\right| \left[\frac{C}{\rho V^\gamma}\right] \qquad [\text{dB/km}] \tag{3.57a}$$

$$\beta_H \Delta\alpha = |\beta_H - \beta_V| = 6 \times 10^5 \;\; F \;\; \left|\frac{(L_1' + L_2') - L_3'}{2}\right| \left[\frac{C}{\rho V^\gamma}\right] \qquad [\text{deg/km}] \tag{3.57b}$$

-Cross-polarisation discrimination (XPD) [25]

The XPD can be given as in Equation 3.47, where m is the ratio between the two linearly polarised waves that produce the circular polarisation and $\phi = 90°$ is the phase difference between them. Both m and ϕ can be determined using Equation 3.48.

C. S. Rai, May, 2012 [10]

Rai [10] followed exactly the same procedure followed by Ghobrial and Sharif [5] to find the attenuation coefficient, phase shift coefficient and XPD of the propagating circularly polarised wave under the assumption of ellipsoidal dust particles.

Rai [10] gave the attenuation equation along axes 1, 2 and 3 to be:

$$\alpha_{i,p,q} = -\frac{\pi}{\lambda} \sum_p \sum_q P_p P_q Im \left[\frac{v(\varepsilon - 1)}{1 + A_{i,p,q}(\varepsilon - 1)}\right] \qquad [\text{dB/km}]\,;\; i = 1, 2, 3 \tag{3.58}$$

Considering a linearly polarised wave, given by: $E\cos\omega t$, is incident on an ellipsoidal dust particle at a canting angle θ as shown in Figure 3.2. Due to the differential attenuation happening while the incident wave propagates in a dusty medium, the incident linearly polarised vector E will be rotated by an angle δ, a depolarisation angle. This angle can be given by [10]:

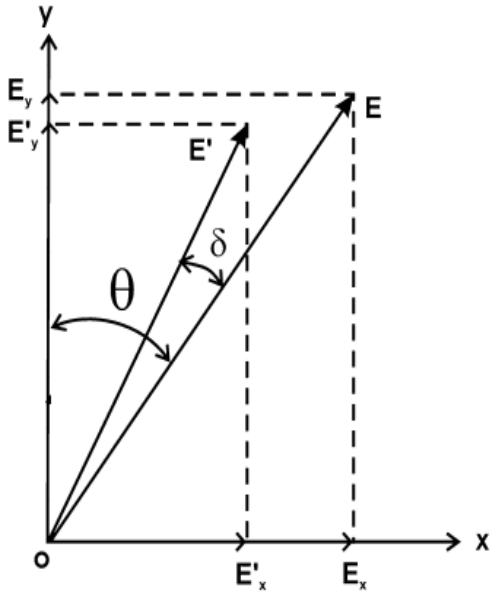

Figure 3.2: Rotation of the linearly polarized field vector due to differential attenuation. [10]

$$\delta = \theta - \tan^{-1}\left(\tan(\theta)\ \log^{-1}\left[\frac{\pi}{40\lambda}\, v\, P_p P_q L \times \sum_p \sum_q \left(\frac{1}{A_{1,p,q} + \frac{1}{\varepsilon - 1}} + \frac{1}{A_{2,p,q} + \frac{1}{\varepsilon - 1}} - \frac{1}{A_{3,p,q} + \frac{1}{\varepsilon - 1}}\right)\right]\right) \tag{3.59}$$

and the XPD can be expressed as [10]:

$$XPD = 20 \log \frac{\sin\ \delta}{\cos\ \delta} \tag{3.60}$$

$$XPD = 20 \log\ \sin\left(\theta - \tan^{-1}\left(\tan(\theta)\ \log^{-1}\left[\frac{\pi}{40\lambda}\ v\ P_p P_q L \times \sum_p \sum_q \left(\frac{1}{A_{1,p,q} + \frac{1}{\varepsilon - 1}} + \frac{1}{A_{2,p,q} + \frac{1}{\varepsilon - 1}} - \frac{1}{A_{3,p,q} + \frac{1}{\varepsilon - 1}}\right)\right]\right)\right) \tag{3.61}$$

The depolarisation loss can be given by [10]:

$$L_d = 10\log\left(1/\cos^2\left\{\theta - \tan^{-1}\left(\tan(\theta)\ \log^{-1}\left[\frac{\pi}{40\lambda}\ v\ P_p P_q L \times \sum_p \sum_q \left(\frac{1}{A_{1,p,q} + \frac{1}{\varepsilon - 1}} + \frac{1}{A_{2,p,q} + \frac{1}{\varepsilon - 1}} - \frac{1}{A_{3,p,q} + \frac{1}{\varepsilon - 1}}\right)\right]\right)\right\}\right) \quad [\text{dB}] \tag{3.62}$$

3.2.2 Limitations of Rayleigh approximations (scattering) [1]

As mentioned in Chapter I, the attenuation due to scattering and absorption is also called extinction. The extinction is defined by Hulst [19] in Equation 3.63. The same definition also apply for the cross-sections.

$$\text{Extinction} = \text{Scattering} + \text{Absorption} \tag{3.63}$$

Vishvakarma and Rai [1] did a theoretical investigation on the main constituents of sand and dust storms, sand, silt and clay. The study revealed that in the lower frequency range, the absorption cross-section is the dominant contributor to the extinction cross-section, while the scattering cross-section has low values at the same frequency range. So, the term responsible for conduction and hence, absorption in the medium, will be appreciably high and the extinction cross-section may be represented by the absorption cross-section. These results are in good agreement with Rayleigh scattering, where the scattering depends on $(\frac{2\pi}{\lambda})^4$.

As the frequency increases, the wavelength will decrease. As a result, the ratio of the particle radius to the incident wavelength will increase. This may enhance the backscatter power from the dust particles and, hence, increase the attenuation as observed by Vishvakarma and Rai [1]. It can be concluded that, as the frequency increases, the scattering cross-section contribution to extinction cross section will also increase, since reducing the wavelength, the term $(\frac{2\pi}{\lambda})^4$ will increase.

This observation is also supported by the radiation theory [1] which states that

the particles exposed to an incident electromagnetic wave should radiate as a dipole. This radiation increases as the incident wave frequency increases. As a result, increasing the frequency of the incident wave increases the scattered, and re-radiated, energy and hence increases the attenuation.

As a conclusion, the attenuation due to dust particles depends on incident wave frequency, dust particles' radii, visibility and the relative dust particles complex permittivity. At higher frequency, it was noticed by the authors that the attenuation prediction using Rayleigh scattering based attenuation models will have a large deviation due to the inherent limitations of Rayleigh scattering assumptions.

According to Goldhirsh [22], Rayleigh scattering-based attenuation models can be used up to 48 GHz. Abdulla [23] concluded in his study that these models can be used up to 37 GHz.

3.2.3 Mie Scattering-Based Model

Due to the limitations of that are caused by the assumptions of Rayleigh scattering, Abdulla et al. [23] and Islam et al. [24], used the first three terms of the Mie extinction formula to develop a mathematical model to predict the attenuation to a propagating electromagnetic wave in a dusty medium. The Mie extinction formula is used to find the attenuation to the propagating particles due to large particles, $\frac{2\pi r}{\lambda} \approx 1$, such as rain drops. Abdulla et al. [23] mention that the main advantage of using the Mie solution as a base to find the electromagnetic wave attenuation is that it takes into account both scattering and absorption of the wave energy by the particles and can be used for high frequencies, higher than 37 GHz, and at high moisture content mediums, more than 10 percent relative humidity .

Oguchi [39] reported that the attenuation to a microwave signal passing through 1 km slab of rain can be given by:

$$A = 4.343 \times 10^3 \int_{r_{min}}^{r_{max}} Q_{ext} n(r) \mathrm{d}r \tag{3.64}$$

where r_{min} and r_{max} are the minimum and maximum dust particles radii in a dust storm and Q_{ext} is the dust particle total extinction cross-section. The Q_{ext} is given by Kerr [27] as:

$$Q_{ext} = \lambda \rho^3 \left(C_1 + C_2 \rho^2 + C_3 \rho^3 \right. \tag{3.65}$$

where $\rho = \frac{2\pi r}{\lambda}$ and $\rho \ll 1$. The constants C_1, C_2 and C_3 are given by:

$$\begin{aligned}
C_1 &= \frac{6\varepsilon''}{(\varepsilon'+2)^2 + \varepsilon''^2} \\
C_2 &= \frac{\varepsilon''}{15} \left\{ 3 \left[\frac{7\varepsilon'^2 + 7\varepsilon''^2 + 4\varepsilon' - 20}{[(\varepsilon'+2)^2 + \varepsilon''^2]^2} \right] + 1 + \frac{25}{[(2\varepsilon'+3)^2 + 4\varepsilon''^2]} \right\} \\
C_3 &= \frac{4}{3} \left\{ \left[\frac{(\varepsilon'-1)^2(\varepsilon'+2)^2 + \varepsilon''^2[2(\varepsilon'-1)(\varepsilon'+2) - 9] + \varepsilon''^4}{[(\varepsilon'+2)^2 + \varepsilon''^2]^2} \right] \right\}
\end{aligned}$$

By substituting Equation 3.65 and the three constant into Equation 3.64, we arrive to the following attenuation equation reported by Abdulla et al. [23] and given by:

$$\begin{aligned}
A = \frac{1.714 \times 10^5}{\lambda} C_1 \int_{r_{min}}^{rmax} r^3 n(r) \mathrm{d}r \\
+ \frac{6769 \times 10^6}{\lambda^3} C_2 \int_{r_{min}}^{rmax} r^5 n(r) \mathrm{d}r \\
+ \frac{4.253 \times 10^7}{\lambda^4} C_3 \int_{r_{min}}^{rmax} r^6 n(r) \mathrm{d}r
\end{aligned} \tag{3.66}$$

Islam et al. [24] simplified the equation to the form:

$$A = 94.3 \; c_1 \frac{r_e}{V\lambda} + 3721.2 \; c_2 \frac{r_e^3}{V\lambda^3} + 23381 \; c_3 \frac{r_e^4}{V\lambda^4} \tag{3.67}$$

which the same equation was achieved by Abdulla et al. [23], but with different equations of the constant C_2 and C_3. Abdulla et al. [23] gave the constants as:

$$\begin{aligned} C_1 &= \frac{6\varepsilon''}{(\varepsilon'+2)^2+\varepsilon''^2} \\ C_2 &= \varepsilon'' \left\{ \frac{6}{5}\left[\frac{7\varepsilon'^2+7\varepsilon''^2+4\varepsilon'-20}{[(\varepsilon'+2)^2+\varepsilon''^2]^2}\right] + \frac{1}{15} + \frac{5}{3\left[(2\varepsilon'+3)^2+4\varepsilon''^2\right]} \right\} \\ C_3 &= \frac{4}{3}\left\{ \left[\frac{(\varepsilon'-1)^2(\varepsilon'+2)+[2(\varepsilon'-1)(\varepsilon'+2)-9]+\varepsilon''^4}{[(\varepsilon'+2)^2+\varepsilon''^2]^2} \right] \right\} \end{aligned}$$

There are two small differences between the constants given by Kerr [27] and Abdulla et al. [23]. In the constant c_2, Abdulla et al. [23] multiplied the first term by 6. In the third constant, in Abdulla et al. [23] a square is missing for the value $(\varepsilon'+2)$. Islam et al. [24] used Equation 3.29 and assumes equisized dust particles in order to simplify the mathematical calculations involved in evaluating the attenuation. Islam et al. [24] assumed the same constants as Abdulla et al. [23]. For the purpose of this report, it is assumed that the constants equations given by Kerr [27] are the right equations.

3.2.4 Effective Material Property Attenuation Model [2]

Xiao et al. [2] derived an attenuation model obtained using the effective material property. It is obtained from the general formulation of the wave propagation constant, based on an equivalent complex permittivity of the storm medium, the mixture of a host material (air) and sand and dust particles and visibility. The equivalent complex relative permittivity of the storm medium is given by:

$$\begin{aligned} \varepsilon_{eq} &= \varepsilon_{air} + \frac{3v\ \varepsilon_{air}\ \frac{\varepsilon_{sd}-\varepsilon_{air}}{\varepsilon_{sd}+2\varepsilon_{air}}}{1-v\ \frac{\varepsilon_{sd}-\varepsilon_{air}}{\varepsilon_{sd}+2\varepsilon_{air}}} \\ &= \varepsilon'_{eq} - j\varepsilon''_{eq} \end{aligned} \tag{3.68}$$

where ε_{eq} is the equivalent complex relative permittivity, ε_{air} is the air relative

dielectric constant and v is the volume fraction occupied by sand and dust in a storm per unit volume, given by Equation 3.23. ε_{sd} is the complex relative permittivity of sand and dust, respectively, given by Xiao [2]. ε' and ε'' are the real and imaginary parts of the equivalent complex relative permittivity.

This model assumed a negligible magnetic loss of the sand and dust storms. The attenuation of transversal EM waves traveling in the storm can be obtained from:

$$\Gamma = \alpha + j\beta = \sqrt{j\omega\mu_0(j\omega\varepsilon_0\varepsilon_{eq})} \qquad [\mathrm{m}^{-1}] \tag{3.69}$$

where Γ is the complex propagation factor and ω is the angular frequency. α and β are the attenuation and the phase shift. ε_0 and μ_0 are the dielectric constant and permeability of air and ε_{eq} is the complex relative permittivity of the sand and dust storm.

The loss tangent of the storm can be expressed by [2]:

$$\tan\delta = \frac{\varepsilon''_{eq}}{\varepsilon'_{eq}} \tag{3.70}$$

where ε' and ε'' are the real and imaginary parts of the equivalent complex relative permittivity.

From the previous two equations, the attenuation and the phase shift can be expressed as

$$A = 8686\,\frac{2\pi}{\lambda}\left[\frac{\varepsilon'_{eq}}{2}\sqrt{1+\tan^2\delta}-1\right]^{1/2} \qquad [\mathrm{dB/km}] \tag{3.71a}$$

$$\Phi = \frac{3.6\times10^5}{\lambda}\left[\frac{\varepsilon'_{eq}}{2}\sqrt{1+\tan^2\delta}+1\right]^{1/2} \qquad [\mathrm{deg/km}] \tag{3.71b}$$

where λ is the wavelength in air.

3.3 Attenuation Models Performance Analysis

3.3.1 Attenuation Measurements

In the literature, only few practical attenuation measurements were performed. Some attenuation measurements, that were done in simulated sand/dust storms environment in the labs, accuracy was poor due to the difficulty to simulate real storms. In 1976, Ahmed [40] performed few attenuation measurements in the lab for free falling dust under gravity effect. This free falling dust is far from being similar to real storms due to the lack of wind and the friction and collision between particles. These measurements were not considered in this study.

Haddad et al. [3], 1983, performed few lab measurements for both natural and simulated dust samples. The natural dust sample was collected from a dust storm at a height of 3 m. All these measurements were done under simulated dust environment in the lab and is not considered for this study because of the reasons mentioned above.

In 1985, Ghobrial et al. [41] performed two attenuation measurements for two communication links 2 GHz and 7.5 GHz respectively. The path length of the first link was 18 km and 20 km for the second link. Authors reported an attenuation of 0.02222 dB/km for the first link and 0.025 dB/km for the second link. The visibility for the first link was reported to be nil and considered to be 5 m in this study. The visibility of the second link was reported to be 0.15 km. The measurement height was not provided for this experiment and assumed to be 27 m for the purpose of this study. Also, the dust moisture contents for both measurement were not reported.

Ghobrial et al [41] reported that Alhafid et al. measured an attenuation of 0.5778 dB/km for 45 km, 11 GHz link with a visibility of 6 km. The attenuation was 0.3333 dB/km for 8 km visibility and 0.2222 dB/km for 10 km visibility. The measurement height was not given and assumed to be 27 m for this study.

Alhaider and Ali [14], 1987, performed experiments to measure the attenuation for 40 GHz, 14 km during nine different dust storms in Riyadh, Saudi Ara-

bia. The visibilities and the recorded attenuations are shown in Table 3.2. The measurement height and the moisture content of the nine dust storms were not reported. For the purpose of this experiment, a measurement height of 27 m is assumed.

Table 3.2: Measured attenuation for 40 GHz, 14 km communication link, 1987. [14]

Visibility (km)	Attenuation (dB)
0.625	2.0
0.682	2.5
1.25	1.4
1.42	1.0
1.61	2.0
2.05	1.4
2.14	1.0
3.75	1.5
3.75	0.7
5.56	0.5

In 1990, Ghobrial and Jervase [42] measured the attenuation of a 10.5 GHz, 25 km communication link during a dense dust storm in Khartoum, Sudan. The receiving antenna was placed 27 m above the ground level. The visibility was reported to be nil and is assumed to be 5 m for this study. The measured attenuation was 0.256 dB/km.

The last measurement that is considered in this study was done in Sudan for a 15 km, 13 GHz communication link by Islam et al. [24]. The measurement height was net reported and assumed to be 27 m as before. The reported visibility was 50 m. The measured attenuation was 0.67 dB/km.

3.3.2 Effective Particles Radii and Dielectric Constants

The effective particles radii for five different dust storms measured by Alhaider et al. [6] at measurement height of 21 m are shown in Table 3.3 for either normal or log-normal distributions. The calculated effective radii for the height 27 m

using Equation 3.72 [6] are shown in the last column of Table 3.3. The mean of the radii at 27 m is 12.484 μm with a standard deviation of 4.1274.

$$r_e = r_{0e}[h/h_0]^{-\gamma_e}; \quad \gamma_e = 0.04 \tag{3.72}$$

Table 3.3: Effective dust particle radii of five dust storms at 21 m high, 1985-1986 [6] and the calculated effective radii at height of 27 m.

Dust storm event	Effective Radius (μm) h = 21 m	Calculated effective Radius (μm) h = 27 m
I	15.45	15.296
II	13.2	14.068
III	11.4	11.286
IV	10.0	9.90
V	13.0	12.870

For the purpose of the analysis, only two effective radii at a measurement height of 27 m are considered maximum and minimum radii. Alhaider et al. [6] found that three of the five dust samples measured at a height of 21 m follow log-normal particles size distribution while the other two follow normal distribution. The two radii chosen for this analysis are for two samples that follow log-normal distribution.

The dielectric constant value is taken from Table 2.8 as follows:

- For 2 GHz: the dielectric constant at 3 GHz is used for 0% and 20.09% moisture content.
- For 7.5 GHz: the average dielectric constants of two dust samples at 8.6 GHz is used for 0% and 3% moisture content respectively.
- For 10.5 GHz and 11 GHz: the dielectric constant measured at 10 GHz given by Bashir and McEwan [34] is used.
- For 13 GHz: the dielectric constant at 14 GHz is used.

- For 40 GHz: the dielectric constant at 37 GHz and about 10% moisture content is used.

3.3.3 Attenuation Models

The models analysed in this study are:

Model 1:

The attenuation models derived by Chu [15], Ansari and Evans [8] and Alhaider et al. [6] are identical. The following equation is used for this model:

$$A = \frac{566.74}{V\lambda} \; r_e \; \left[\frac{\varepsilon''}{(\varepsilon'+2)^2 + \varepsilon''^2}\right] \qquad \text{[dB/km]} \tag{3.73}$$

Model 2:

The models derived by Gobrial and Sharif [5], Goldhirsh [22], Yan [38] and Dong et al. [25] are identical. The values $\rho = 2.44 \times 10^3$ [kg/m^3], $C = 2.3 \times 10^{-5}$ [kg.km/m^3] and $\gamma = 1.7$, applicable for Sudan, are used in this analysis. This model equation is:

$$A = \frac{2.316 \times 10^{-3}}{\lambda V^{\gamma}} \; \left[\frac{\varepsilon''}{(\varepsilon'+2)^2 + \varepsilon''^2}\right] \qquad \text{[dB/km]} \tag{3.74}$$

Model 3:

Nevertheless the assumption of applying Mie solution to find the attenuation due to dust particles is theoretically invalid. Here, the model developed by Abdulla [23] and modified by Islam et al. [24] and based on the Mie solution is

compared with the other attenuation models to evaluate its performance. The model equation is:

$$A = 94.3\ c_1 \frac{r_e}{V\lambda} + 3721.2\ c_2 \frac{r_e^3}{V\lambda^3} + 23381\ c_3 \frac{r_e^4}{V\lambda^4} \tag{3.75}$$

and the constants are given by Kerr [27]:

$$\begin{aligned} C_1 &= \frac{6\varepsilon''}{(\varepsilon'+2)^2+\varepsilon''^2} \\ C_2 &= \frac{\varepsilon''}{15}\left\{3\left[\frac{7\varepsilon'^2+7\varepsilon''^2+4\varepsilon'-20}{[(\varepsilon'+2)^2+\varepsilon''^2]^2}\right]+1+\frac{25}{[(2\varepsilon'+3)^2+4\varepsilon''^2]}\right\} \\ C_3 &= \frac{4}{3}\left\{\left[\frac{(\varepsilon'-1)^2(\varepsilon'+2)^2+\varepsilon''^2[2(\varepsilon'-1)(\varepsilon'+2)-9]+\varepsilon''^4}{[(\varepsilon'+2)^2+\varepsilon''^2]^2}\right]\right\} \end{aligned}$$

Model 4:

The last model included in this analysis is the attenuation model that is based on the effective material property and developed by Xiao et al. [2]. The equivalent complex relative permittivity of a dust storm is given by:

$$\begin{aligned} \varepsilon_{eq} &= \varepsilon_{air} + \frac{3v\ \varepsilon_{air}\ \frac{\varepsilon_{sd}-\varepsilon_{air}}{\varepsilon_{sd}+2\varepsilon_{air}}}{1-v\ \frac{\varepsilon_{sd}-\varepsilon_{air}}{\varepsilon_{sd}+2\varepsilon_{air}}} \\ &= \varepsilon'_{eq} - j\varepsilon''_{eq} \end{aligned} \tag{3.76}$$

Here also the values applicable for Sudan are used to evaluate the volume fraction. The attenuation model is given by:

$$A = 8686\,\frac{2\pi}{\lambda}\left[\frac{\varepsilon'_{eq}}{2}\sqrt{1+\tan^2\delta}-1\right]^{1/2} \qquad \text{[dB/km]} \tag{3.77}$$

where δ is the storm loss tangent and given by:

$$\tan\delta = \frac{\varepsilon''_{eq}}{\varepsilon'_{eq}} \tag{3.78}$$

3.3.4 Predicted Attenuations vs Measurements

For the purpose of validating the predicted attenuations by different models against the available measurements, the attenuation is calculated for the minimum and maximum particles radii at a height of 27 m as shown in Table 3.3. As the measurement heights, for the performed experiments, are not reported except for the experiment by Ghobrial and Jervase [42] which is reported as 27 m. So, the measurement height chosen for this analysis is 27 m as it is reported by one experiment and it is a reasonable height for a communication tower.

Tables 3.4 and 3.5 show the Predicted attenuation for maximum and minimum particles radii at a measurement height of 27 m. These predicted values are compared with the measurements. These results are discussed in Section 3.3.7

Table 3.4: Predicted vs measured attenuations using effective radius of $r_e = 15.296\mu$m at a measurement height of 27 m.

			Calculated Attenuation							
Freq. (GHZ)	Visibility (km)	Measured Attenuation [dB/km]	Dielectric Constant	Model 1	%Error	Model 2	%Error	Model 3	%Error	Model 4	%Error
2	0.005	0.0222	$2.27 - j0.0341$[1]	0.0216	2.70	0.0084	62.16	0.0216	2.70	0.0084	62.16
2	0.005	0.0222	$11.3 - j2.825$[2]	0.1766	695.5	0.0684	208.1	0.1763	694.1	0.0683	207.7
7.5	0.150	0.0250	$4.71 - j0.1175$[3]	0.0038	84.80	0.0012	95.20	0.0038	84.80	0.0011	95.60
7.5	0.150	0.0250	$5.565 - j0.451$[4]	0.0113	54.80	0.0035	86	0.0113	54.80	0.0035	86
10.5	0.005	0.2560	$5.33 - j0.285$[5]	0.3214	25.55	0.1244	51.41	0.3209	25.35	0.1244	51.41
11	6.0	0.5778	$5.33 - j0.285$[5]	2.8×10^{-4}	99.95	6.6×10^{-5}	99.99	2.8×10^{-4}	99.95	6.6×10^{-5}	99.99
11	8.0	0.3333	$5.33 - j0.285$	2.1×10^{-4}	99.94	4.9×10^{-5}	99.99	2.1×10^{-4}	99.94	4.9×10^{-5}	99.99
11	10.0	0.2222	$5.33 - j0.285$	1.7×10^{-4}	99.92	3.8×10^{-5}	99.99	1.7×10^{-4}	99.92	3.7×10^{-5}	99.99
13	0.050	0.670	$5.50 - j1.3$[6]	0.1686	74.84	0.0555	91.72	0.1683	74.88	0.0555	91.72
40	0.625	2.00	$3.2 - j0.8$[7]	0.0534	97.33	0.0148	99.26	0.0534	97.33	0.0148	99.26
40	0.682	2.50	$3.2 - j0.8$	0.0490	98	0.0134	99.50	0.0489	98	0.0134	99.50
40	1.250	1.40	$3.2 - j0.8$	0.0267	98.10	0.0070	99.50	0.0267	98.10	0.0070	99.50
40	1.420	1.00	$3.2 - j0.8$	0.0235	97.65	0.0061	99.39	0.0235	97.65	0.0061	99.39
40	1.610	2.00	$3.2 - j0.8$	0.0207	98.97	0.0054	99.73	0.0207	98.97	0.0054	99.73
40	2.050	1.40	$3.2 - j0.8$	0.0163	98.84	0.0041	99.71	0.0163	98.84	0.0041	99.71
40	2.140	1.00	$3.2 - j0.8$	0.0156	98.44	0.0040	99.60	0.0156	98.44	0.0040	99.60
40	3.750	0.70	$3.2 - j0.8$	0.0089	98.73	0.0022	99.69	0.0089	98.73	0.0022	99.69
40	5.560	0.50	$3.2 - j0.8$	0.0060	98.80	0.0014	99.72	0.0060	98.80	0.0014	99.72

1: Dielectric constant at 3 GHz and 0% moisture content.
2: Dielectric constant at 3 GHz and 20.09% moisture content.
3: Dielectric constant at 8.6 GHz and 0% moisture content, average for two samples.
4: Dielectric constant at 8.6 GHz and 3% moisture content, average for two samples.
5: Dielectric constant at 10 GHz and unknown moisture content.
6: Dielectric constant at 14 GHz and unknown moisture content.
7: Dielectric constant at 37 GHz and >10% moisture content.

Table 3.5: Predicted vs measured attenuations using effective radius of $r_e = 9.90\mu$m at a measurement height of 27 m.

			Calculated Attenuation							
Freq. (GHZ)	Visibility (km)	Measured Attenuation [dB/km]	Dielectric Constant	Model 1	%Error	Model 2	%Error	Model 3	%Error	Model 4	%Error
2	0.005	0.0222	$2.27 - j0.0341$[1]	0.0140	36.94	0.0084	62.16	0.0140	2.70	0.0084	36.94
2	0.005	0.0222	$11.3 - j2.825$[2]	0.1143	414.9	0.0684	208.1	0.1763	694.1	0.1141	414
7.5	0.150	0.0250	$4.71 - j0.1175$[3]	0.0024	90.40	0.0012	95.20	0.0038	84.80	0.0024	90.40
7.5	0.150	0.0250	$5.565 - j0.451$[4]	0.0073	70.80	0.0035	86	0.0113	54.80	0.0073	70.80
10.5	0.005	0.2560	$5.33 - j0.285$[5]	0.2080	18.75	0.1244	51.41	0.3209	25.35	0.2077	18.87
11	6.0	0.5778	$5.33 - j0.285$[5]	1.8×10^{-4}	99.97	6.6×10^{-5}	99.99	1.8×10^{-4}	99.97	6.6×10^{-5}	99.99
11	8.0	0.3333	$5.33 - j0.285$	1.4×10^{-4}	99.96	4.9×10^{-5}	99.99	1.4×10^{-4}	99.96	4.9×10^{-5}	99.99
11	10.0	0.2222	$5.33 - j0.285$	1.1×10^{-4}	99.94	3.8×10^{-5}	99.99	1.1×10^{-4}	99.94	3.7×10^{-5}	99.99
13	0.050	0.670	$5.50 - j1.3$[6]	0.1091	83.72	0.0555	91.72	0.1089	83.75	0.0555	91.72
40	0.625	2.00	$3.2 - j0.8$[7]	0.0346	98.27	0.0148	99.26	0.0345	98.28	0.0148	99.26
40	0.682	2.50	$3.2 - j0.8$	0.0317	98.73	0.0134	99.50	0.0317	98.73	0.0134	99.50
40	1.250	1.40	$3.2 - j0.8$	0.0173	98.76	0.0070	99.50	0.0173	98.76	0.0070	99.50
40	1.420	1.00	$3.2 - j0.8$	0.0152	98.48	0.0061	99.39	0.0152	98.48	0.0061	99.39
40	1.610	2.00	$3.2 - j0.8$	0.0134	99.33	0.0054	99.73	0.0134	99.33	0.0054	99.73
40	2.050	1.40	$3.2 - j0.8$	0.0105	99.25	0.0041	99.71	0.0105	99.25	0.0041	99.71
40	2.140	1.00	$3.2 - j0.8$	0.0101	99	0.0040	99.60	0.0101	99	0.0040	99.60
40	3.750	0.70	$3.2 - j0.8$	0.0058	99.17	0.0022	99.69	0.0058	99.17	0.0022	99.69
40	5.560	0.50	$3.2 - j0.8$	0.0039	99.22	0.0014	99.72	0.0039	99.22	0.0014	99.72

1: Dielectric constant at 3 GHz and 0% moisture content.
2: Dielectric constant at 3 GHz and 20.09% moisture content.
3: Dielectric constant at 8.6 GHz and 0% moisture content, average for two samples.
4: Dielectric constant at 8.6 GHz and 3% moisture content, average for two samples.
5: Dielectric constant at 10 GHz and unknown moisture content.
6: Dielectric constant at 14 GHz and unknown moisture content.
7: Dielectric constant at 37 GHz and >10% moisture content.

3.3.5 Predicted attenuation vs Visibility

As the visibility is a very important factor in the attenuation prediction for all models, Figure 3.3 shows that the predicted attenuation to a 10 GHz incident wave decreases with the visibility. The visibility in this plot ranges between 5 m to 500 m. The particles' effective radii of 9 μm is used here.

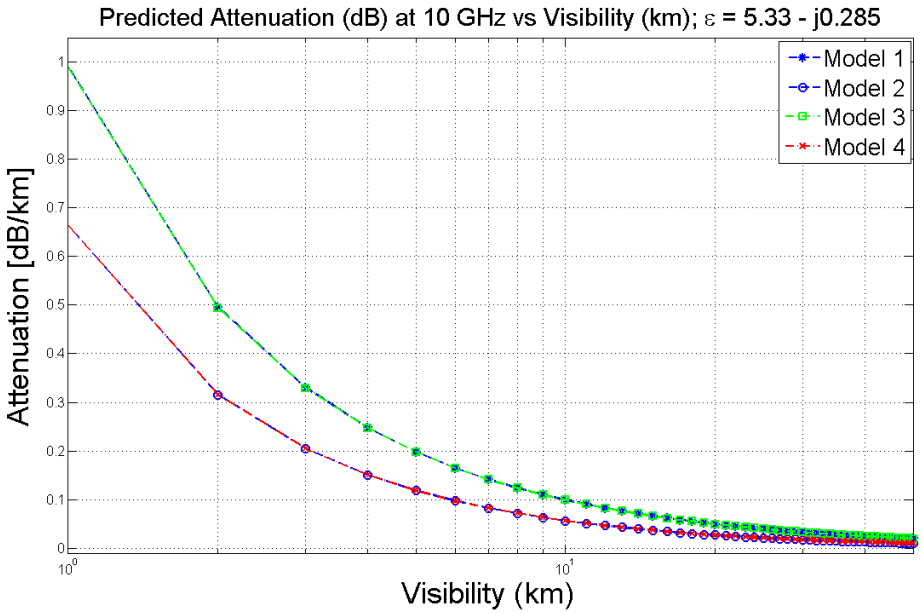

Figure 3.3: Models predicted attenuation vs visibility

3.3.6 Predicted Attenuation vs Measurement Height

The receiver (measurement) height is an important factor when designing communication links or when choosing a radar deployment site. The relation between measurement height and the predicted attenuation is investigated. The visibility is believed to vary directly with the height following the relation given by Sharif [4] as:

$$V = V_0 \left[\frac{h}{h_0}\right]^{(0.28/\gamma)} \tag{3.79}$$

where V is the visibility at desired height h, V_0 is the reference visibility at reference height h_0, $\gamma = 1.07$, the value that is found to be applicable for Sudan, is assumed. Using the above equation, Figure 3.4 shows how the predicted attenuation of different models varies with the measurement height.

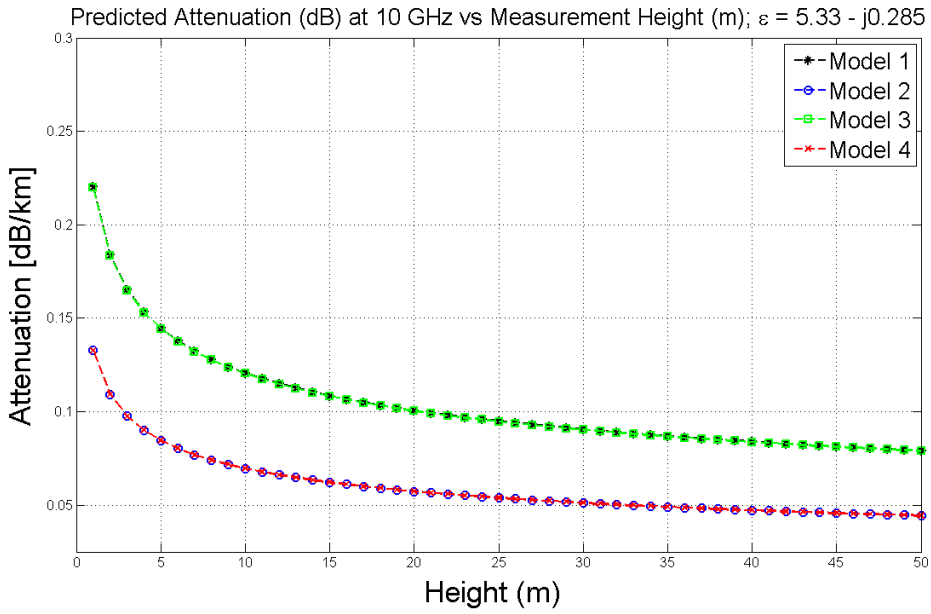

Figure 3.4: Models predicted attenuation vs height

3.3.7 Discussion

Ghobrial et al. [41], Ghobrial and Jervase [42] and Alhaider and Ali [14] used the visibility data reported by airports' meteorological stations. In the first two references, the visibility was reported to be "nil". This visibility data has a degree of inaccuracy which enhances the errors involved with the attenuation predictions. In addition, Ghobrial and Jervase [42] collected 20 graduate students, who live in different parts of Khartoum, Sudan, in the next day of dense dust storm event and asked them how far they could see during that dust storm. The visibility data recorded by the meteorological stations are not accurate enough to be used for accurate attenuation predictions for an electromagnetic wave propagating through a dusty medium. As a result of using this visibility data, the

predicted attenuation will have some errors. For example, the high visibility together with the high attenuation reported by Alhafid [41] increases the suspicion on the accuracy of the visibility measurements. The methods used to measure the visibility in the rest of the discussed measurements are not specified. An accurate means of measuring the visibility should be used in future in order to increase the attenuation predictions accuracy.

The moisture contents of all dust storms events analysed in this section were not reported by the authors. The dusty medium moisture content has a huge effect on the medium dielectric constant. For example, the dielectric constant of a dust sample measured at 3 GHz with 20.09% moisture content is about five times double the value for dry dust. As a result, the huge impact of the dusty medium moisture content on the dielectric constant cannot be ignored. In this study, measured dielectric constants at different moisture content and different frequencies were used to predict the attenuation. In cases where the dielectric constant at the experimented frequency is lacking, the dielectric constant measured at the nearest frequency is used. This may increase the error in predicted attenuation and hence the error percentage when compared to measurements.

Tables 3.4 and 3.5 show the measured attenuations and the attenuations predicted by different models. Due to the lack of the dielectric constant at certain frequencies, the dust dielectric constant measured at the nearest frequency to the frequency under test is used. This forms another factor that affects the attenuation predictions accuracy.

In the two tables, at some frequencies, 2 GHz and 7.5 GHz, two dielectric constants, measured for two dust samples with different moisture contents, are used to show how severe the change of the dielectric constant to the predicted attenuation value. The first row of the two tables gives the predicted attenuation at 2 GHz and dielectric constant measured for dust sample at 3 GHz with 0% moisture content and the second row for 20.09% moisture content. The predicted attenuations using the dielectric constant of a dust sample with 20.09% moisture content is approximately eight times double that of the once predicted using the dielectric constant for dry dust. At 7.5 GHz, the dielectric constant measured

for dry dust samples and samples with 3% moisture content at 8.6 GHz are used. The predicted attenuation using the dielectric constant of samples with 3% moisture content is approximately three times double the attenuations predicted for dry dust. This demonstrates the importance of using the right dielectric constant of the dusty medium that is measured at the right moisture content in order to achieve better attenuation predictions.

Table 3.4 gives the measured predicted attenuations for incident signals with different frequencies assuming the largest, 15.296μm, effective dust particles radius. The very high error in the second row is due to the use of a dielectric constant measured for dust sample with 20.09% moisture content. In general, the errors between the measurements and the predictions increase with the incident wave frequency. This proved the limitations of Rayleigh approximation at high frequencies as discussed in Chapter II. The predicted attenuation, also, increases with the increase of the moisture content of the medium, as it increases the dielectric constant. Similar observations were noticed in Table 3.5 which was simulated with dust particles' effective radii of 9.90μm. It can be noticed from both tables that predicted attenuations of the model derived from the Mie solution, Model 3, using the constants given by Kerr [27], are identical to those predicted by the model developed by Chu [15], Model 1. Model 2 and 4 also give identical predictions.

The predicted attenuations for the larger particles effective radius is approximately 1.5 times more than the one for the smaller particles effective radius, and as discussed in previous chapters, the particles radii become smaller as the measurement height increases. As a result, the higher the measurement, the lower the attenuation.

Figure 3.3 shows an exponential decay of the attenuation predictions as the visibility increases. As can be seen the model developed by Chu [15], Model 1, and the model developed using the Mie solution, Model 3, using the constants equation provided by Kerr [27], gave identical result of the predicted attenuations for a 10 GHz propagating signal. The other two models, Model 2 and Model 4, gave identical results. The last two models predict lower attenuations compared

to the first two. All models exponentially decay as the visibility increases.

The attenuation predictions of all the four models decay exponentially with the measurement height as shown in Figure 3.4. As the height factor is not directly included in any of the attenuation models, Equation 3.79 was used to find the visibilities from height. The reference height, h_0, used to generate this plot is 1.5 meters with reference visibility of 5 m. The constant γ is taken to be 1.07. As before, models 1 and 3 are identical and the same applies to models 2 and 4. It can be concluded that the higher that measurements, the lower the attenuation.

As can be seen from the figures, Models 2 and 4 predict 25% to 40% lower attenuation than Models 1 and 3 at very low visibility and height. The difference becomes lower as the visibility or the measurement height increases.

3.4 Conclusions

Scattering and absorption are the two main mechanisms that cause the attenuation of the propagating electromagnetic wave in dusty mediums, i. e. when interacting with dust particles. The wave scattering by dust particles falls under the Rayleigh scattering type because the ratio of the particles radii to the incident signal wavelength, size parameter is much smaller than 1.

Eight attenuation models discussed in this chapter assume that all the dust particles have spherical shapes. The relation between optical attenuation and the visibility is derived using the mean value of the threshold contrast as assumed by Chu [15]. Six out of eight models are based on the validity of Rayleigh approximation for dust particles, i.e. fall in the Rayleigh scattering regime. Ansari and Evans [8] proved this assumption by calculating the scattering amplitude using exact method and a method that uses Rayleigh approximation for 100 μm particles, sand particles, at 37 GHz. The calculations reveal that only a negligible difference between the two methods which prove the validity of Rayleigh approximation.

Ghobrial and Sharif [5] consider the air volume fraction that is occupied by dust

while deriving the attenuation model. They used the empirical constants that are applicable for Sudan in their derivation. In this model, similar to the other models, the attenuation is inversely proportional to the visibility. Ansari and Evans [8] modified the attenuation prediction model to cater for particles size distribution of the exponential type reported by Ghobrial for Sudan.

In nature, the dust particles shapes vary randomly between needle-like to sphere or disc and are very rarely to be found in perfect sphere shapes. Ghobrial and Sharif [5], as an extension to their attenuation model, assume the dust particles to have ellipsoidal shapes with different axes ratios. This assumption provides three degrees of freedom and is a realistic approximation to dust particles in nature. The attenuation prediction using this model is assumed to increase the prediction accuracy over the attenuation models that assume spherical dust particles. The disadvantages of the attenuation prediction models based on the assumption of ellipsoidal dust particles are that the mathematical complexity increases, large mathematical calculations are required, and the attenuation is evaluated based on the incident wave polarisation. Rai [10] derived the additional loss caused by the depolarisation which enhances the attenuation.

When the incident wave frequency increases, the wavelength decreases, Vishvakarma and Rai [1] observed that the attenuation predictions by Rayleigh scattering-based models are associated with a large deviation due to the inherent limitations of Rayleigh approximation. Abdulla et al. [23] suggested 37 GHz as the maximum frequency limit for the use of Rayleigh scattering-based models. Goldhirsh [21] suggested 48 GHz.

Due to Rayleigh scattering-based attenuation prediction models, Abdulla et al. [23] used the first few terms of the well-known Mie extinction formula to develop a mathematical attenuation prediction model for a wave propagating in a dusty medium. The solution of the Mie extinction formula is used to predict the wave attenuation due to large particles such as rain and ice, when the size parameter can be approximated by 1. The size parameter for the largest dust particles can be approximated to 1 for frequencies above 400 GHz. This makes the use of the Mie extinction formula theoretically invalid.

The constants used in the attenuation prediction formula that was given by Abdulla et al. [23] and Islam et al. [24] led to overestimation of the attenuation. By replacing these constants equations by the equations given by Kerr [27] for the same constants, the performance of the Mie scattering-based model become identical to the model developed by Chu [15], which assumes the applicability of Rayleigh approximation.

The attenuation model derived by Xiao et al. [2], which is based on the effective material property, provides identical results to the model derived by Ghobrial and Sharif [5].

The attenuation prediction by all the models decay exponentially with increasing the visibility or the height. In general, the model developed by Chu and the Mie scattering-based model give identical performance. Also, the effective material property attenuation prediction model gives identical attenuation prediction to the model derived by Ghobrial and Sharif [5]. The first two models' predictions are higher than the second two models predictions. The attenuation predictions increase with the effective dust particles' radii.

In order to increase the attenuation prediction accuracy, we must:

- Use an accurate mean to measure the visibility.
- Measure the dielectric constant of dust storms together with measuring the moisture content of the dust storm.
- Experimentally, determine the dielectric constants for wide range of frequencies of the incident waves and for all possible moisture content of dust storms.

Chapter 4

Charged Sand/Dust Particles Attenuation Effects

The mathematical attenuation prediction models, based on pure dielectric scattering, underestimate the attenuation that occurs to an electromagnetic wave propagating through a dusty medium, as shown in Section 3.3. Haddad et al. [3] measured an attenuation of 34 dB/km of 9.35 GHz wave propagating through a 60 gm/m^3 dense simulated dust storm. The mathematical prediction using the Chu [15] model gives an attenuation of 1 dB/km. For another simulated dust storm, by Haddad et al. [3], with visibility of 4.06 metres, the measured attenuation was 17 dB/km while the predicted attenuation was 0.8 dB/km.

This suggested more research required to find other factors that led to the high attenuation. In the last century, many researchers - refer to Zheng et al. [26] -, through some observation and some experiments, found that one of the main reasons for this high attenuation is the electric charges gained by the particles during the wind-blown storms. The first section of this chapter provides a brief review of wind-blown sand/dust electrification. Section 4.2, is about the effects of the charged particles on the electromagnetic wave propagating in the dusty medium containing these particles. One mathematical attenuation prediction model is provided. The last section of this chapter discusses the effect of the dust particles' size distribution, taking exponential distribution as an example,

on the mathematical attenuation model given in the previous section.

4.1 Wind-Blown Sand/Dust Electrification

Many authors (Rudge 1913 and 1914; Gill 1948; Kunkel 1950; Latham 1964; Karma 1969; Stow 1969; Greeley and Leach 1978) are aware, by observations and experiments, of the ability of the sand/dust particles in a wind-blown storm to gain electric charges [26] [43]. Some of the above-mentioned authors reported that the electric field measured in a wind-blown sand/dust storms is higher the one measured for clear air [26].

Experiments by Rudge revealed that the large (sand) particles gain positive charges while the small (dust) particles gain negative charges. Shaw, 1929, blew sand through a sandpaper sheath at room temperature. His finding was that the blown sand became negatively charged and the sandpaper became positively charged. [26]

Gill, 1948, observed the discharge (spark) phenomenon in the wind-blown sand/dust storms. Later, by experiment, he found that the small particles acquired positive charges and the large particles gained negative charges. In 1949, Paterson found that the sand particles in a storm gain negative charges. [26] [43]

Latham, 1964, assumed that the friction and the collision between different sizes particles in sand/dust storms are the two main sources of charges [43]. Greeley and Leach, 1979, found that the dust particles with radii less than 30 μm acquired negative charges and the larger particles acquired positive charges [26] [43].

In 1993 and 1998, Schmidt and Dent observed that the electric field in a wind-blown sand/dust storm is vertical to the earth's surface pointing upward. They measured the magnitude for a storm at a height of 1.7 m and found it to be up to 166 kV/m. They found that the charged particles are the main cause for this electric field. [43].

Recently, Zheng et al. [26] [43] verified the sand/dust particles electrification by

means of simulated dust storms in a dust tunnel. For detailed experiments and results refer to [26] and [43]. The experiments revealed that the small (dust) particles gain negative charges during a wind-blown sand/dust storm. The acquired charges by the particles became more negative as the wind speed decreases.

Another finding was that the charges on the particles became more negative as the measurement height increases for the a constant wind speed. This result agreed with Schmidt and Dent findings.

4.2 Attenuation due to Charged Sand/Dust Particles

4.2.1 Medium Equisized Spherical Particles

As discussed in the previous chapter, the dust storms attenuate the electromagnetic waves propagating through them. This attenuation weakens the signal to a degree where the signal might disappear.

As the electrification of dust particles is proven in the previous section, the electric charges play a major role in increasing the attenuation for the propagating wave. Zhou et al. [11], investigated the attenuation due to charged particles and derived a mathematical attenuation prediction model that took the particles' charges into account. Zhou et al. [11] assume that the dust sand/dust storm is a monodispersive system, all the particles have the same radii, and that the electric charge on each sand/dust particle is distributed only on the spherical top cap of the particle as shown in Figure 4.1. E_0 is the incident electric field and $2\theta_0$ is the charge distribution angle on the particle surface.

As is clear from the figure, the authors assume spherical particles that satisfy Rayleigh approximation requirement. Using Equations 3.2 and 3.4, Zhou et al. [11] give the attenuation as:

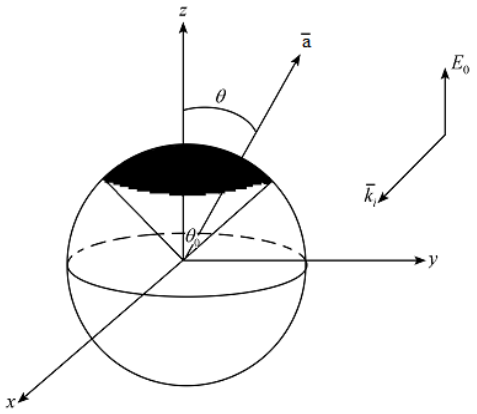

Figure 4.1: A charged sand/dust particle with incident wave. [11]

$$A = \frac{54.576}{\lambda}\left[-\frac{135\ r}{13\ V}\left(\frac{\varepsilon''}{(\varepsilon'+2)^2+\varepsilon''^2}\right)+\frac{15r^2\rho\, q\sin^2\theta_0}{26V\varepsilon E_0\,(1-\cos\theta_0)}Im(\varepsilon_d-1)\right] \quad \text{[dB/km]} \tag{4.1}$$

where λ is the wavelength of the incident wave in metres, r is the particle radius, V is the visibility, ε' and ε'' are the real and imaginary parts of the sand/dust dielectric constant, ρ is the particle mass density [kg/m^3], q is the charge to mass ratio [μ C/kg], ε is the electric permitivity of air and ε_d is the dielectric constant of sand/dust. This result is identical to the one achieved by Qunfeng et al. [44].

4.2.2 Medium with Particles Size Distribution

Exponential Distribution [44]

Analysis of the sand/dust particles in Sudan, as reported by Ansari and Evans [8], revealed that the particles' radii follow an exponential vertical distribution of the type:

$$P(r) = \beta exp(-\beta r) \tag{4.2}$$

with a mean value $\overline{a} = 1/\beta$.

The attenuation due to charged particles following exponential size distribution is expressed by Qungeng et al. [44] as:

$$A = \frac{2\pi}{\lambda}\left[-\frac{135}{\beta V}\left(\frac{\varepsilon''}{(\varepsilon'+2)^2+\varepsilon''^2}\right)+\frac{30\ \rho\, q\sin^2\theta_0}{\beta^2 V\varepsilon E_0\,(1-\cos\theta_0)}Im(\varepsilon_d-1)\right] \quad [\text{dB/km}] \tag{4.3}$$

Uniform, Exponential, Rayleigh and Log-normal Distributions [45]

As the complex dielectric constant is a function of particles' moisture content and the incident wave frequency, Dong and Xu [45] utilises the well-known mixing rule derived from the Maxwell-Garnett equation to evaluate the complex equivalent dielectric constant. The equivalent dielectric constant can be given by [45]:

$$\begin{aligned}\varepsilon_m^* &= \varepsilon_s + \frac{3p\ \frac{\varepsilon_w-\varepsilon_s}{\varepsilon_w+2\varepsilon_s}}{1-p\ \frac{\varepsilon_w-\varepsilon_s}{\varepsilon_w+2\varepsilon_s}} \\ &= \varepsilon'_m - j\varepsilon''_m\end{aligned} \tag{4.4}$$

where ε_m^* is the equivalent complex dielectric constant of the sand particle, ε_s and ε_w are the dielectric constants of dry sand/dust and water respectively and p is the water content volume percentage.

According to one particles size distribution analysis performed in Sudan, the particles' radii follow distribution of the type [45]:

$$N(r) = N_0 p(r) \tag{4.5}$$

where N_0 is the number of particles per unit volume and $p(r)$ is the probability density function.

The attenuation to an electromagnetic wave propagating through a dusty medium

can be given as [45]:

$$A = \frac{2.097 \times 10^3}{\lambda V}\left[-\left(\frac{3\varepsilon''_m}{(\varepsilon'_m+2)^2+\varepsilon''^2_m}\right)\cdot\frac{I_3}{I_2}+\frac{\rho\, q(\varepsilon^*_m-1)\sin^2\theta_0}{6\varepsilon E_0\,(1-\cos\theta_0)}\cdot\frac{I_4}{I_2}\right] \quad [\text{dB/km}] \tag{4.6}$$

where $I_n = \int_0^\infty r^n p(r)$ and $n = 1, 2, 3, 4$. The two ratios can be found as [45]:

Uniform Distribution

The distribution can be given by:

$$p(r) = \frac{1}{2a} \tag{4.7}$$

where a is the average. The ratios are:

$$I_3/I_2 = 3a/2 \tag{4.8a}$$
$$I_4/I_2 = 12a^2/5 \tag{4.8b}$$

Exponential Distribution

The distribution can be given by:

$$p(r) = \frac{1}{a}\exp(-r/a) \tag{4.9}$$

The ratios are:

$$I_3/I_2 = 3a \tag{4.10a}$$
$$I_4/I_2 = 12a^2 \tag{4.10b}$$

Rayleigh Distribution

The distribution can be written as:

$$p(r) = \frac{r}{\sigma^2} \exp(-r/2\sigma^2) \tag{4.11}$$

The average "a" is: $a = \sigma\sqrt{\pi/2}$ and σ is the standard deviation. The ratios are:

$$I_3/I_2 = 3a/2 \tag{4.12a}$$
$$I_4/I_2 = 8a^2/\pi \tag{4.12b}$$

Log-normal Distribution

The distribution can be written as:

$$p(r) = \frac{1}{r\sigma\sqrt{2\pi}} \exp(-\frac{(\ln r - \mu)^2}{2\sigma^2}) \tag{4.13}$$

The average is given as: $a = \exp(\mu + \sigma^2/2)$ and μ is the mean. The standard deviation can be given as: $\sigma = a\sqrt{(\exp\sigma^2 - 1)}$. The ratios are:

$$I_3/I_2 = a(1+\delta^2); \quad \delta = \sigma/a \tag{4.14a}$$
$$I_4/I_2 = a(1+\delta^2)^{5/2} \tag{4.14b}$$

4.3 Conclusions

Various indoor and out door experiments on the sand/dust storms prove the electrification of sand/dust particles in wind-blown storms. The amount of charge on each particle depends on many factors such as: particle size, wind speed

and measurement height. The charge on each particle is distributed on the top spherical cap of the particle. The knowledge of both the charge amount and its distribution angle on each particle is required to accurately predict the attenuation. The wind speed and the measurement height have huge effects on the amount of charge on the particle. The attenuation models for both monodispersive and polydispersive systems are given. The attenuation equations for several particles size distributions are presented.

Several factors affect the electrification process and the quantity of charges that accumulate on dust particles such as: geographical origin of the dust storm and its geographical location, wind speed and the measurement height. Mathematical attenuation prediction models, for both monodispersive systems and polydispersive systems with different dust particles size distribution are presented in this chapter.

The loss mechanism due to charged dust particles is not explained by the dielectric scattering models available in the literature. The existence of the electric charges on the dust particles' surface is a valid reason, but not the only one, to explain the high measured attenuations in the literature compared to the available attenuation prediction theoretical models.

The electrification of the dust particles in dust storms is a real problem for electromagnetic wave propagating through and requires further investigation. As both the charge amount and its distribution angle on each particle are difficult to measure experimentally, further future work is required to tackle this problem and to produce mathematical attenuation prediction models that consider the dust particles electrification effect.

Finding the amount of charge and the distribution angle on each particle is a difficult task to be accomplished. These measurements should be done for each storm with different speed, different geographical area or different measurement height. This leads to the impracticality of including the charge effect when predicting the attenuation.

Chapter 5

Conclusions and Recommendations

The main objective of this research was to study all mathematical attenuation prediction models available in the literature for predicting the attenuation to electromagnetic waves propagating in dusty mediums. Then to validate these models against the few practical attenuation measurement available in the literature and to see the applicability of these models to radar applications.

The conclusions drawn after performing the above-mentioned study are presented in the next section. The conclusions are followed by some recommendations for future work.

5.1 Conclusions

The dust is composed of silt and clay particles with radii of less than 50 μm. The shapes of the dust particles are random and irregular without any particular symmetry. They may vary from needle-like to disc, sphere or ellipse.

Most of the attenuation prediction models that predict the attenuation to an electromagnetic wave propagating in a dusty medium, assume spherical dust

particles as this assumption enhances the mathematical simplicity of the models.

The assumption that the dust particles are ellipsoids provide three degrees of freedom and give more realistic approximation to real dust particles. Different ellipse axes ratios result in wide variety of shapes. Another advantage of this assumption is that it accounts for one extra loss that results from interaction between the incident wave and the dust particle, which is the depolarisation loss. However, the depolarisation loss should be evaluated for each dust particle. The only side-effect of this assumption is that it increases the model's computational complexity as it requires the evaluation of depolarisation factors along each ellipse axis and it requires the evaluation of depolarisation loss. It is believed that the assumption of ellipsoid dust particles will give more accurate attenuation prediction, but this has not been proved in practice.

The dust particles get smaller as the height increases, following vertical size distribution. Many particles size distribution functions were reported in the literature such as: straight line, exponential, power low, normal and log-normal. Only one experiment were performed at a measurement height of 21 m and revealed that distribution at that height is either normal or log-normal. As the particle size become smaller with the height, the attenuation will decrease as the dust particles' radii is involved in the attenuation calculation. A practical experiment revealed that the attenuation at a height of 21 m is 20 - 55% lower than the attenuation measured at 1 m high.

The difficulties involved in measuring the optical attenuation and the dust mass concentration, as they are required to predict the attenuation, leads to the use of visibility, or the optical visibility, as it is easy to measure and is related to both factors. As the visibility increases, the attenuation will decrease. The visibility, also, increases with the height.

The dusty medium dielectric constant is a critical factor when evaluating attenuation predictions as it can change the attenuation value greatly. All the dielectric constant measurements available in the literature were done in the laboratories for collected dust samples. Only one attenuation prediction model, based on effective material property, considered the use of a well-known mixing rule to

find the dielectric constant of the air-dust mixture, dust storm. Not considering the evaluation of the dielectric constant of the air-dust mixture may enhance the error in attenuation prediction.

A factor that can largely change the value of the dielectric constant, and hence the attenuation, is the dust moisture content. This conclusion is drawn from the effect of collected dust samples moisture content on the laboratory measured dielectric constants. The frequency of the incident wave can change the dielectric constant value.

Six of the eight attenuation mathematical prediction models are based on the assumption of the validity of the Rayleigh assumption. This assumption is mathematically valid for the tiny dust particles. As demonstrated in Chapter III, there is a very small difference in the calculation of the forward scattering amplitude between the Rayleigh-based method and the exact calculation for a 100 μm sand particle, larger than the dust particle which proves the validity of Rayleigh assumption.

As the incident wave frequency increases, the attenuation predicted by Rayleigh approximation-based models start to deviate largely. This is assumed to be an effect of the assumption of Rayleigh approximation. It was then suggested to use the first few terms of the well-known Mie solution, which is used for rain attenuation calculation, to derive an attenuation prediction model that has less deviated attenuation predictions at high frequencies. Theoretically, the Mie solution can be used only for large particles such as large sand grains and raindrops, not with the tiny dust particles. By ignoring the constants given by this model's developers and using the constants equations given by Kerr [27], this model gave a comparable result to the first developed attenuation prediction model that is based on Rayleigh assumption.

The first attenuation prediction model developed by Chu [15] and the model derived from Mie solution gave identical results. The model based on the effective material property gave identical attenuation predictions to the models - that utilise the volume fraction of the air occupied by dust in a dust storm and the relation between dust density and the visibility. All four models predictions

decay exponentially with both visibility and height. The first two models gave higher attenuation predictions compared to the second two models. It was also observed, both experimentally and theoretically, that the attenuation increases with increasing dust particles' effective radii.

The attenuation predictions by all four models are very small compared to the available measurements. This high difference between the two may be due to:

- In accurate visibility measurements.
- Unavailability of accurate dielectric constant measurements for wide range of frequencies and wide range of moisture content.

Another reason that might explain the high measured attenuation is the presence of electrical charges on the dust particles surface. Several experiments prove the process of electrification of the wind-blown dust particles in dust storms mainly due to the interaction between particles. The loss mechanism due to charged dust particles is not explained by the dielectric scattering models that are available in the literature. It can be concluded that the electrification of the dust particles is a valid reason that might explain the high measured attenuations compared to those predicted mathematically.

The mathematical attenuation prediction models developed taking the charge on the dust particles into account are not practically validated. They are also not practical as they depend on the knowledge of the charge's amount in each particle as well as the charge's distribution angle on the top cap of the particle. These two factors are impossible to measure practically. These models might work if a reasonable assumption is made for both factors.

5.2 Recommendations

Based on the study conclusions above, several recommendations for future work are made in order to improve the theoretical models' predictions or develop a

new attenuation prediction model that is based on accurate measurements. The recommendations are:

Visibility

- Accurate means to measure the visibility, or the optical visibility, should be used. More accurate means to measure the visibility can be found specially with the vast development in the technology. This will increase the mathematical prediction models accuracy as the visibility form an important factor in the attenuation prediction process.

Dielectric constant

- Accurate means should be used to measure both dielectric constant and the moisture content of real dust storms. The measured dielectric constant should be then compared with the values given in the literature for collected dust samples that are measured inside the laboratories. This will give an idea about the difference between the laboratory measurement and the real dust storm measurement in order to evaluate the possibility of doing future dielectric constant measurement in the laboratories.

- The relation between the dielectric constant and the humidity in the air, given by a mathematical equation, should be validated. This will help in finding the dielectric constant values when changes in humidity, and hence moisture content, occur without having to repeat the practical experiment.

- The dielectric constant measurements should be performed over a wide frequency band as the frequency is one of the main contributors to the dielectric constant value. The same applies for doing the measurements for several moisture contents. This will help in building a good database that contains the values of dielectric constant for several scenarios.

Dust density and the constants γ and C

- A geographical study should be performed in the area of interest to find the applicable values of the two constants γ and C.

- A study should be performed on the dust density in a storm and its relation with the wind speed, soil type and the geographical area affected by the dust storm in order to increase the attenuation prediction model's accuracy.

Attenuation measurements

- Attenuation measurements should be performed over a wide frequency range using accurate means. This will help in validating the mathematical attenuation prediction model and may help in developing an empirical attenuation prediction model if the pure theoretical models fail to achieve reasonable predictions.

Effect of charges on dust particles

- The effect of electric charges distributed on the surface of the dust particles on the attenuation should be investigated. This may requires some measurements of the electric charges, both in the lab and during real dust storms. Due to the difficulties in measuring the charges on each dust particle and how they are distributed, an empirical attenuation prediction model may be required. Many attenuation measurements in several environmental scenarios and several geographical locations will help in increasing the accuracy of any empirical model.

Appendix A

EBE Faculty: Assessment of Ethics in Research Projects

Any person planning to undertake research in the Faculty of Engineering and the Built Environment at the University of Cape Town is required to complete this form before collecting or analysing data. When completed it should be submitted to the supervisor (where applicable) and from there to the Head of Department. If any of the questions below have been answered YES, and the applicant is NOT a fourth year student, the Head should forward this form for approval by the Faculty EIR committee: submit to Ms Zulpha Geyer (Zulpha.Geyer@uct.ac.za; Chem Eng Building, Ph 021 650 4791). Students must include a copy of the completed form with the final year project when it is submitted for examination.

Name of Principal Researcher/Student: Saad Alhuwaimel

Department: ELECTRICAL ENGINEERING

If a Student: YES **Degree:** M.Eng (Radar) **Supervisor:** Michael Inggs

f a Research Contract indicate source of funding/sponsorship: NA

Research Project Title: Study of Radar Signal Attenuation in Dust storms

Overview of ethics issues in your research project:

Question 1: Is there a possibility that your research could cause harm to a third party (i.e. a person not involved in your project)?	NO
Question 2: Is your research making use of human subjects as sources of data?	NO
Question 3: Does your research involve the participation of or provision of services to communities?	NO
Question 4: If your research is sponsored, is there any potential for conflicts of interest?	NO

If you have answered YES to any of the above questions, please append a copy of your research proposal, as well as any interview schedules or questionnaires (Addendum 1) and please complete further addenda as appropriate.

I hereby undertake to carry out my research in such a way that:

- there is no apparent legal objection to the nature or the method of research; and
- the research will not compromise staff or students or the other responsibilities of the University;
- the stated objective will be achieved, and the findings will have a high degree of validity;
- limitations and alternative interpretations will be considered;
- the findings could be subject to peer review and publicly available; and
- I will comply with the conventions of copyright and avoid any practice that would constitute plagiarism.

Signed by:

	Full name and signature	Date
Principal Researcher/Student:	Saad Alhuwaimel	21 December 2012

This application is approved by:

	Full name and signature	Date
Supervisor (if applicable):	Michael Inggs	21 December 2012
HOD (or delegated nominee):	Janine Buxey	21 December 2012

Bibliography

[1] B. Vishvakarma and C. Rai, "Limitations of rayleigh scattering in the prediction of millimeter wave attenuation in sand and dust storms," in *Geoscience and Remote Sensing Symposium, 1993. IGARSS'93. Better Understanding of Earth Environment., International*, pp. 267–269, IEEE, 1993.

[2] X.-Y. Dong, H.-Y. Chen, and D.-H. Guo, "Microwave and millimeter-wave attenuation in sand and dust storms," *Antennas and Wireless Propagation Letters, IEEE*, vol. 10, pp. 469 –471, 2011.

[3] S. Haddad, M. Salman, and R. Jha, "Effects of dust/sandstorm on some aspects of microwave propagation," in *ESA Special Publication*, vol. 194, pp. 153–162, 1983.

[4] S. M Sharif, "Dust storms properties related to microwave signal propagation," *Khartoum University Engineering Journal*, vol. 1, no. 1, 2011.

[5] S. Ghobrial and S. Sharief, "Microwave attenuation and cross polarization in dust storms," *Antennas and Propagation, IEEE Transactions on*, vol. 35, no. 4, pp. 418–425, 1987.

[6] A. Ahmed, A. Ali, and M. Alhaider, "Airborne dust size analysis for tropospheric propagation of millimetric waves into dust storms," *Geoscience and Remote Sensing, IEEE Transactions on*, vol. GE-25, pp. 593 –599, sept. 1987.

[7] S. M. Sharif, "Dust particles-size distribution," in *Geoscience and Remote Sensing Symposium, 1987. IGARSS'87. Better Understanding of Earth Environment., International*, IEEE, 1987.

[8] A. Ansari and B. Evans, "Microwave propagation in sand and dust storms," *Communications, Radar and Signal Processing, IEE Proceedings F*, vol. 129, no. 5, pp. 315–322, 1982.

[9] S. Sharif and S. Ghobrial, "X-band measurements of the dielectric constant of dust," in *Proc. Ursi Commission F*, pp. 143–147, 1983.

[10] C. Rai, "Depolarization of millimeter wave due to non-spherical dust particles in storms," *Indian Journal of Physics*, pp. 1–6, 2012.

[11] Q. He, Y. Zhou, and X. Zheng, "Effects of charged sand on electromagnetic wave propagation and its scattering field," *Science in China Series G: Physics Mechanics and Astronomy*, vol. 49, no. 1, pp. 77–87, 2006.

[12] M. Alhaider, "Design considerations for millimeter wave radio links in arid land," *International journal of infrared and millimeter waves*, vol. 7, no. 10, pp. 1559–1570, 1986.

[13] E. Patterson and D. Gillette, "Measurements of visibility vs mass-concentration for airborne soil particles," *Atmospheric Environment (1967)*, vol. 11, no. 2, pp. 193–196, 1977.

[14] M. Alhaider and A. Ali, "Experimental studies on millimeterwave and infrared propagation in arid land: The effect of sand storms," in *Antennas and Propagation, 1989. ICAP 89., Sixth International Conference on (Conf. Publ. No. 301)*, pp. 268–270, IET, 1989.

[15] T. Chu, "Effects of sandstorms on microwave propagation," *Bell Syst. Tech. J*, vol. 58, no. 2, pp. 549–555, 1979.

[16] E. Norinpel, "Microwave attenuation due to dust and sand storm in earth-satellite link," in *Strategic Technology, 2007. IFOST 2007. International Forum on*, pp. 599–601, IEEE, 2007.

[17] M. A. A. Moutaz Al-Dabbas and R. Al-Khafaji, "The mineralogical and micro-organisms effects of regional dust storms over middle east region," *International Journal of Water Resources and Arid Environments*, vol. 1, no. 2, pp. 129–141, 2011.

[18] Z. Elshaikh, I. Rafiqul, O. Khalifa, and H. Abd-El-Raouf, "Mathematical model for the prediction of microwave signal attenuation due to duststorm," *Progress In Electromagnetics Research M*, vol. 6, pp. 139–153, 2009.

[19] H. Hulst and H. Van De Hulst, *Light scattering by small particles*. Dover Pubns, 1957.

[20] S. Patil, M. Koledintseva, R. Schwartz, and W. Huebner, "Prediction of effective permittivity of diphasic dielectrics using an equivalent capacitance model," *Journal of Applied Physics*, vol. 104, no. 7, pp. 074108–074108, 2008.

[21] J. Goldhirsh, "A parameter review and assessment of attenuation and backscatter properties associated with dust storms over desert regions in the frequency range of 1 to 10 ghz," *Antennas and Propagation, IEEE Transactions on*, vol. 30, no. 6, pp. 1121–1127, 1982.

[22] J. Goldhirsh, "Attenuation and backscatter from a derived two-dimensional duststorm model," *Antennas and Propagation, IEEE Transactions on*, vol. 49, no. 12, pp. 1703–1711, 2001.

[23] S. Abdulla, H. Al-Rizzo, and M. Cyril, "Particle-size distribution of iraqi sand and dust storms and their influence on microwave communication systems," *Antennas and Propagation, IEEE Transactions on*, vol. 36, no. 1, pp. 114–126, 1988.

[24] M. ISLAM, Z. OMER ELSHAIKH, O. KHALIFA, A. ALAM, S. KHAN, and A. NAJI, "Prediction of signal attenuation due to duststorms using mie scattering," *IIUM Engineering Journal*, vol. 11, no. 1, pp. 71–87, 2010.

[25] Q. Dong, L. Yingle, J. Xu, H. Zhang, and W. Jun, "Effect of sand and dust storms on microwave propagation," 2011.

[26] X. Zheng, *Mechanics of wind-blown sand movements*. Springer, 2009.

[27] D. Kerr, *Propagation of short radio waves*, vol. 24. Peter Peregrinus Limited, 1951.

[28] A. Ahmed, A. Ali, and M. Alhaider, "Measurement of atmospheric particle size distribution during sand/duststorm in riyadh, saudi arabia," *Atmospheric Environment (1967)*, vol. 21, no. 12, pp. 2723–2725, 1987.

[29] D. Rowe, M. Nouh, K. Al-Dhowalia, and M. Mansour, "Indoor-outdoor relationship of suspended particulate matter in riyadh, saudi arabia," *Journal of the Air Pollution Control Association*, vol. 35, no. 1, pp. 24–26, 1985.

[30] M. Sviridenkov, D. Gillette, A. Isakov, I. Sokolik, V. Smirnov, B. Belan, M. Pachenko, A. Andronova, S. Kolomiets, V. Zhukov, *et al.*, "Size distributions of dust aerosol measured during the soviet-american experiment in tadzhikistan, 1989," *Atmospheric Environment. Part A. General Topics*, vol. 27, no. 16, pp. 2481–2486, 1993.

[31] S. Ghobrial, "Crosspolarization and attenuation in earth-satellite links due to dust storms," in *Antennas and Propagation Society International Symposium, 1984*, vol. 22, pp. 633 – 636, jun 1984.

[32] S. Sharif, "Performance of earth-satellite links during dust storms at the x-band," *SES Journal*, vol. 40, no. 33, pp. 14–19, 1993.

[33] W. Hinds, "Aerosol technology: properties, behavior, and measurement of airborne particles," 1982.

[34] S. Bashir and N. McEwan, "Microwave propagation in dust storms: a review," in *Microwaves, Antennas and Propagation, IEE Proceedings H*, vol. 133, pp. 241–247, IET, 1986.

[35] S. Ghobrial, "Effect of hydroscopic water on dielectric constant of dust at x-band," *Electronics Letters*, vol. 16, no. 10, pp. 393–394, 1980.

[36] Y. Ruike, W. Zhensen, and Y. Jinguang, "The study of mmw and mw attenuation considering multiple scattering effect in sand and dust storms

at slant paths," *International Journal of Infrared and Millimeter Waves*, vol. 24, no. 8, pp. 1383–1392, 2003.

[37] J. Stratton, *Electromagnetic theory*, vol. 33. Wiley-IEEE Press, 1941.

[38] Y. Yan, "Microwave propagation in saline dust storms," *International journal of infrared and millimeter waves*, vol. 25, no. 8, pp. 1237–1243, 2004.

[39] T. Oguchi, "Electromagnetic wave propagation and scattering in rain and other hydrometeors," *Proceedings of the IEEE*, vol. 71, no. 9, pp. 1029–1078, 1983.

[40] I. Ahmed, *Microwave propagation through sand and dust storms*. PhD thesis, PhD Thesis, University of Newcastle Upon Tyne, UK, 1976.

[41] S. Ghobrial, M. Hemeidi, and M. Tawfig, "Observations on 2 and 7.5 ghz microwave links during dust storms," *Electronics Letters*, vol. 23, no. 1, pp. 44–45, 1987.

[42] S. Ghobrial and J. Jervase, "Microwave propagation in dust storms at 10.5 ghz¡ cd02821. gif¿ a case study in khartoum, sudan¡ cd02821. gif¿," *IEICE transactions on communications*, vol. 80, no. 11, pp. 1722–1727, 1997.

[43] X. Zheng, N. Huang, and Y. Zhou, "Laboratory measurement of electrification of wind-blown sands and simulation of its effect on sand saltation movement," *Journal of Geophysical Research*, vol. 108, no. D10, p. 4322, 2003.

[44] D. Qunfeng, X. Jiadong, L. Yingle, and W. Mingjun, "Microwave propagation in charged sand particles," in *Antennas Propagation and EM Theory (ISAPE), 2010 9th International Symposium on*, pp. 379–382, IEEE, 2010.

[45] Q. Dong and J. Xu, "Effects of charged particles size distribution on microwave propagation in sandstorms," *Journal of Electromagnetic Waves and Applications*, vol. 25, no. 2-3, pp. 315–325, 2011.